Department of Radio Science and Engineering

Functional Metasurfaces

Younes Ra'di

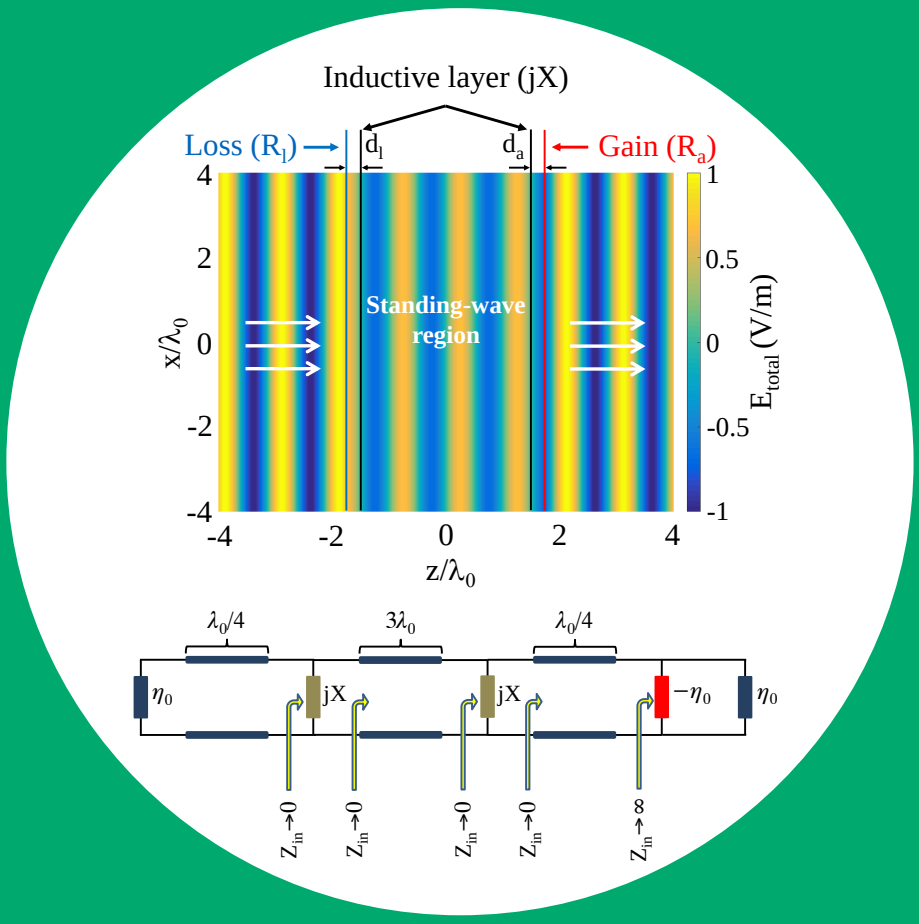

Aalto University

DOCTORAL DISSERTATIONS

Aalto University publication series
DOCTORAL DISSERTATIONS 211/2015

Functional Metasurfaces

Younes Ra'di

A doctoral dissertation completed for the degree of Doctor of Science (Technology) to be defended, with the permission of the Aalto University School of Electrical Engineering, at a public examination held at the lecture hall S1 of the school on 18 December 2015 at 14:00.

Aalto University
School of Electrical Engineering
Department of Radio Science and Engineering

Supervising professor
Professor Sergei Tretyakov, Aalto University, Finland

Preliminary examiners
Professor Maria Kafesaki, University of Crete, Greece
Professor Anthony Grbic, University of Michigan, USA

Opponent
Professor Stefano Maci, University of Siena, Italy

Aalto University publication series
DOCTORAL DISSERTATIONS 211/2015

ISBN 978-952-60-6566-3 (printed)
ISBN 978-952-60-6567-0 (pdf)
ISSN-L 1799-4934
ISSN 1799-4934 (printed)
ISSN 1799-4942 (pdf)
http://urn.fi/URN:ISBN:978-952-60-6567-0

Unigrafia Oy
Helsinki 2015

Finland

441 697
Printed matter

Aalto University

Abstract

Aalto University, P.O. Box 11000, FI-00076 Aalto www.aalto.fi

Author
Younes Ra'di

Name of the doctoral dissertation
Functional Metasurfaces

Publisher School of Electrical Engineering

Unit Department of Radio Science and Engineering

Series Aalto University publication series DOCTORAL DISSERTATIONS 211/2015

Field of research Radio Engineering

Manuscript submitted 1 September 2015 **Date of the defence** 18 December 2015

Permission to publish granted (date) 9 November 2015 **Language** English

☐ **Monograph** ☒ **Article dissertation (summary + original articles)**

Abstract

This thesis studies the use of functional metasurfaces composed of single arrays of polarizable unit cells in order to manipulate electromagnetic waves. The main topics that are studied are absorbing metasurfaces, metamirrors, Huygens' metasurfaces, and parity-time-symmetric metasurfaces.

In the first part of the thesis, we introduce the general theory of off-band-transparent absorbing metasurfaces. First, we consider metasurfaces which symmetrically absorb electromagnetic waves hitting any of their sides. As an example for symmetric absorbing metasurfaces, we introduce a novel off-band-transparent light absorber composed of a single array of core-shell particles. We continue this study by introducing the concept of asymmetric absorbing metasurfaces. We study single-layer sheets which work as total absorbers only from one side and investigate what functionalities can be engineered for illumination from the opposite side.

The second part of the thesis is devoted to the concept of off-band-transparent reflecting metasurfaces. We consider both symmetric and asymmetric metamirrors. We show how arrays of electrically small resonant bianisotropic particles can be employed to fully reflect electromagnetic plane waves hitting any of their sides while enabling independent and full control over the phase of waves reflected from their different sides.

The third part of the thesis focuses on the concept of Huygens' metasurfaces. We first present the concept of symmetric and asymmetric transparent metasurfaces. We introduce one-way transparent metasurfaces which offer controllable functionalities for waves hitting their non-transparent sides. We furthermore introduce the concept of all-angle Huygens' metasurfaces. These metasurfaces are reflectionless for any arbitrary input wavefront while enabling manipulation of transmitted waves in unprecedented ways.

In the last part of the thesis, we study the concept of parity-time-symmetric metasurfaces. Utilizing these metasurfaces, it is shown how electromagnetic plane waves can be fully recreated behind a highly reflecting metallic screen. The proposed structure works as a new form of one-dimensional cloak which is capable of cloaking an almost fully reflective metallic screen in both spectrally and angularly selective manner.

Keywords Metasurfaces, Absorbers, Reflectors, Transparency, Bianisotropy, Parity-time symmetry

ISBN (printed) 978-952-60-6566-3 **ISBN (pdf)** 978-952-60-6567-0

ISSN-L 1799-4934 **ISSN (printed)** 1799-4934 **ISSN (pdf)** 1799-4942

Location of publisher Helsinki **Location of printing** Helsinki **Year** 2015

Pages 119 **urn** http://urn.fi/URN:ISBN:978-952-60-6567-0

Preface

This thesis summarizes selected results obtained at the Department of Radio Science and Engineering of Aalto University under the supervision of Prof. Sergei Tretyakov.

My warmest thanks and gratitude go to my supervisor, Prof. Sergei Tretyakov, for accepting me as a doctoral student and for his trust, encouragement, and guidance during these years. You have been a tremendous mentor for me. I would like to thank you for allowing me to grow as a research scientist. Your advice on both research as well as on my career have been priceless.

I would also like to thank Prof. Constantin Simovski. I very much appreciate many discussions I had with you on some of research works included in this thesis.

In full gratitude I would like to acknowledge all my co-authors, colleagues, and all staff members in the Department of Radio Science and Engineering, especially the present and former members of our scientific group: Dr. Igor Nefedov, Dr. Pekka Alitalo, Dr. Antti Karilainen, Dr. Constantinos Valagiannopoulos, Dr. Dmitry Morits, Dr. Mohammad Albooyeh, Mr. Teemu Niemi, Mr. Joni Vehmas, Mr. Viktar Asadchy, Mr. Mohammad Sajjad Mirmoosa, Mr. Mikhail Omelyanovich, Mr. Sergei Kosulnikov, Mr. Pavel Voroshilov, Ms. Svetlana Tcvetkova, and Mr. Amr Elsakka.

I wish to thank Prof. Maria Kafesaki and Prof. Anthony Grbic for accepting to review this thesis.

My sincere gratitude and special thanks for all the joint work, discussions, and guidance go to Prof. Constantin Simovski, Prof. Andrea Alù, Prof. Richard Ziolkowski, Prof. Ari Sihvola, Dr. Andrey Osipov, Dr. Iñigo Liberal, Dr. Dimitrios Sounas, Mr. Viktar Asadchy, and Mr. Dimitris Tzarouchis.

During this thesis work I have received financial support from the Aalto ELEC Doctoral School, the Nokia Foundation, and the HPY Research Foundation. All this support is most gratefully acknowledged.

Words cannot express how grateful I am to my mother, brother, mother-in-law, and father-in-law for all of the sacrifices that they have made on my behalf. Thank you for your support and encouragement during the whole course of my studies.

Finally, but most importantly, I wish to thank my beloved wife Hoda, for all her love, constant support, and bringing so much happiness into my life. Your encouragement, patience, and unwavering love were undeniably the bedrock upon which the past five years of my life have been built.

Espoo, November 16, 2015,

Younes Ra'di

Contents

List of Publications

This thesis consists of an overview and of the following publications which are referred to in the text by their Roman numerals.

I Y. Ra'di, V. S. Asadchy, S. U. Kosulnikov, M. M. Omelyanovich, D. Morits, A. V. Osipov, C. R. Simovski, and S. A. Tretyakov. Full light absorption in single arrays of spherical nanoparticles. *ACS Photonics*, vol. 2, no. 5, pp. 653–660, April 2015.

II Y. Ra'di, V. S. Asadchy, and S. A. Tretyakov. Total absorption of electromagnetic waves in ultimately thin layers. *IEEE Trans. Antennas Propag.*, vol. 61, no. 9, pp. 4606–4614, September 2013.

III Y. Ra'di, V. S. Asadchy, and S. A. Tretyakov. Tailoring reflections from thin composite metamirrors. *IEEE Trans. Antennas Propag.*, vol. 62, no. 7, pp. 3749–3760, July 2014.

IV Y. Ra'di, V. S. Asadchy, and S. A. Tretyakov. One-way transparent sheets. *Phys. Rev. B*, vol. 89, no. 7, p. 075109, February 2014.

V Y. Ra'di and S. A. Tretyakov. Angularly-independent Huygens' metasurfaces. **In** *IEEE International Symposium on Antennas and Propagation and North American Radio Science Meeting*, Vancouver, Canada, pp. 874–875, July 2015.

VI Y. Ra'di, D. L. Sounas, A. Alù, and S. A. Tretyakov. Parity-time symmetric tunnelling. **In** *Metamaterials' 2015: The Ninth International*

Congress on Advanced Electromagnetic Materials in Microwaves and Optics, Oxford, UK, pp. 500–502, September 2015.

Author's Contribution

Publication I: "Full light absorption in single arrays of spherical nanoparticles"

The idea for the paper came from Prof. Sergei Tretyakov and Dr. Andrey Osipov. The design and simulations for the narrowband absorber were carried out by the author together with Dr. Dmitry Morits. The ideas for three other absorbing metasurface designs were proposed by the author. The author mainly carried out the designs, simulations, and writing the paper under supervision of Prof. Sergei Tretyakov.

Publication II: "Total absorption of electromagnetic waves in ultimately thin layers"

The idea for the paper was proposed by Prof. Sergei Tretyakov. The analytical derivations were all done by the author together with Mr. Viktar Asadchy. All the co-authors contributed in writing the paper. The work was conducted under supervision of Prof. Sergei Tretyakov.

Publication III: "Tailoring reflections from thin composite metamirrors"

The idea for the paper came from Prof. Sergei Tretyakov. The analytical derivations and simulations were all done by the author and then verified by Mr. Viktar Asadchy. All the co-authors contributed in writing the paper. The work was conducted under supervision of Prof. Sergei Tretyakov.

Publication IV: "One-way transparent sheets"

The idea for the paper was proposed by Prof. Sergei Tretyakov. The analytical derivations and simulations were all done by the author together with Mr. Viktar Asadchy. All the co-authors contributed in writing the paper. The work was conducted under supervision of Prof. Sergei Tretyakov.

Publication V: "Angularly-independent Huygens' metasurfaces"

The idea for the paper came from Prof. Sergei Tretyakov. The analytical derivations, simulations, and writing the paper were all done by the author under supervision of Prof. Sergei Tretyakov.

Publication VI: "Parity-time symmetric tunnelling"

The idea for the paper came from Profs. Sergei Tretyakov and Andrea Alù. The designs, simulations, and writing the paper were all done by the author under supervision of all other co-authors.

List of Abbreviations

OBT	Off-band-transparent
$\mathcal{PT}$	Parity-time
TE	Transverse electric
TM	Transverse magnetic
2D	Two-dimensional
3D	Three-dimensional

List of Symbols

a	Array period [m]
a_1	Electric dipolar term of the Mie series expansion
b_1	Magnetic dipolar term of the Mie series expansion
c	Speed of light in vacuum [ms^{-1}]
d	Array period [m] (All chapter but chapter 5)
d	Thickness of the layer [m] (Only in chapter 5)
d_l	Distance between the lossy and inductive layers [m]
d_a	Distance between the active and inductive layers [m]
$\mathbf{E}$	Electric field due to the source [Vm^{-1}]
$\mathbf{E}_\mathrm{av}$	Surface-averaged tangential electric field over the metasurface plane [Vm^{-1}]
$\mathbf{E}_\mathrm{loc}$	Local electric field [Vm^{-1}]
$\mathbf{E}_\mathrm{inc}$	Incident electric field [Vm^{-1}]
$\mathbf{E}_\mathrm{r}$	Reflected electric field [Vm^{-1}]
$\mathbf{E}_\mathrm{t}$	Transmitted electric field [Vm^{-1}]
$\mathbf{H}$	Magnetic field due to the source [Am^{-1}]
$\mathbf{H}_\mathrm{av}$	Surface-averaged tangential magnetic field over the metasurface plane [Am^{-1}]
$\mathbf{H}_\mathrm{loc}$	Local magnetic field [Am^{-1}]
$\mathbf{H}_\mathrm{inc}$	Incident magnetic field [Am^{-1}]
$\overline{\overline{I}}$	Three-dimensional unit dyadic
$\overline{\overline{I}}_\mathrm{t}$	Two-dimensional unit dyadic
i	Imaginary unit
$\overline{\overline{J}}_\mathrm{t}$	Vector-product operator
$\mathbf{J}_\mathrm{e}$	Electric surface current density [Am^{-1}]
$\mathbf{J}_\mathrm{m}$	Magnetic surface current density [Vm^{-1}]
j	Imaginary unit
$\mathbf{k}_\mathrm{t}$	Tangential component of the wave vector of the incident plane wave [m^{-1}]

k_t	Length of the tangential component of the wave vector [m^{-1}]
k_0	Free-space wavenumber [m^{-1}]
$\mathbf{m}$	Magnetic dipole moment [Vms]
$\mathbf{n}$	Unit vector normal to the metasurface
$\mathbf{p}$	Electric dipole moment [Ams]
p	Period of the holes [m]
$\overline{\overline{R}}$	Reflection coefficient tensor
R	Reflection coefficient
$R_{-\mathbf{z}_0}$	Reflection coefficient for the $-\mathbf{z}_0$-directed incident wave
$R_{+\mathbf{z}_0}$	Reflection coefficient for the $+\mathbf{z}_0$-directed incident wave
R_TM	Reflection coefficient for the TM case
R_TE	Reflection coefficient for the TE case
R_l	Resistance of the lossy layer [Ω]
R_a	Resistance of the active layer [Ω]
r_Ag	Radius of the silver core [m]
r	Radius of the holes [m]
S	Metasurface unit cell area [m^2]
$\overline{\overline{T}}$	Transmission coefficient tensor
t	Time [s]
$t_\mathrm{n-Si}$	Thickness of the amorphous n-doped silicon shell [m]
$\mathbf{v}\cdot\mathbf{w}$	Scalar product of two vectors $\mathbf{v}$ and $\mathbf{w}$
$\mathbf{v}\times\mathbf{w}$	Vector product of two vectors $\mathbf{v}$ and $\mathbf{w}$
$\mathbf{vw}$	Dyadic product of two vectors $\mathbf{v}$ and $\mathbf{w}$
V	Individual moving coupling coefficient [sm^2]
$\widehat{V}$	Effective moving coupling coefficient [sm^2]
$\overline{\overline{Z}}_\mathrm{e}$	Dyadic electric surface impedance normalized to the free-space impedance η_0
$\overline{\overline{Z}}_\mathrm{m}$	Dyadic magnetic surface impedance normalized to the free-space impedance η_0
$Z_\mathrm{e,m}^\mathrm{TM}$	Electric/magnetic surface impedance normalized to the free-space impedance η_0 for the TM polarized incident wave
$Z_\mathrm{e,m}^\mathrm{TE}$	Electric/magnetic surface impedance normalized to the free-space impedance η_0 for the TE polarized incident wave
$\mathbf{z}_0$	Unit vector normal to the metasurface
$\overline{\overline{\widehat{\alpha}}}_\mathrm{ee}$	Effective electric polarizability tensor [$\mathrm{Asm}^2\ \mathrm{V}^{-1}$]
$\overline{\overline{\widehat{\alpha}}}_\mathrm{em}$	Effective electromagnetic polarizability tensor [sm^2]
$\overline{\overline{\widehat{\alpha}}}_\mathrm{me}$	Effective magnetoelectric polarizability tensor [sm^2]
$\overline{\overline{\widehat{\alpha}}}_\mathrm{mm}$	Effective magnetic polarizability tensor [$\mathrm{A}^{-1}\mathrm{sm}^2\mathrm{V}$]

$\overline{\overline{\alpha}}_{\mathrm{ee}}$ Individual electric polarizability tensor [Asm^2 V^{-1}]

$\overline{\overline{\alpha}}_{\mathrm{em}}$ Individual electromagnetic polarizability tensor [sm^2]

$\overline{\overline{\alpha}}_{\mathrm{me}}$ Individual magnetoelectric polarizability tensor [sm^2]

$\overline{\overline{\alpha}}_{\mathrm{mm}}$ Individual magnetic polarizability tensor [A^{-1}sm^{2}V]

$\widehat{\alpha}_{\mathrm{ee}}^{\mathrm{co}}$ Co-component of effective electric polarizability tensor [Asm^2 V^{-1}]

$\widehat{\alpha}_{\mathrm{ee}}^{\mathrm{cr}}$ Cross-component of effective electric polarizability tensor [Asm^2 V^{-1}]

$\widehat{\alpha}_{\mathrm{em}}^{\mathrm{co}}$ Co-component of effective electromagnetic polarizability tensor [sm^2]

$\widehat{\alpha}_{\mathrm{em}}^{\mathrm{cr}}$ Cross-component of effective electromagnetic polarizability tensor [sm^2]

$\widehat{\alpha}_{\mathrm{me}}^{\mathrm{co}}$ Co-component of effective magnetoelectric polarizability tensor [sm^2]

$\widehat{\alpha}_{\mathrm{me}}^{\mathrm{cr}}$ Cross-component of effective magnetoelectric polarizability tensor [sm^2]

$\widehat{\alpha}_{\mathrm{mm}}^{\mathrm{co}}$ Co-component of effective magnetic polarizability tensor [A^{-1}sm^{2}V]

$\widehat{\alpha}_{\mathrm{mm}}^{\mathrm{cr}}$ Cross-component of effective magnetic polarizability tensor [A^{-1}sm^{2}V]

α_{ee} Individual electric polarizability [Asm^2 V^{-1}]

α_{mm} Individual magnetic polarizability [A^{-1}sm^{2}V]

$\alpha_{\mathrm{ee}}^{\mathrm{co}}$ Co-component of individual electric polarizability [Asm^2 V^{-1}]

$\alpha_{\mathrm{em}}^{\mathrm{cr}}$ Cross-component of individual electromagnetic polarizability [sm^2]

$\alpha_{\mathrm{me}}^{\mathrm{cr}}$ Cross-component of individual magnetoelectric polarizability [sm^2]

$\alpha_{\mathrm{mm}}^{\mathrm{co}}$ Co-component of individual magnetic polarizability [A^{-1}sm^{2}V]

$\overline{\overline{\beta}}_{\mathrm{e}}$ Electric interaction constant tensor

$\overline{\overline{\beta}}_{\mathrm{m}}$ Magnetic interaction constant tensor

ϵ_0 Vacuum permittivity [Asm^{-1}V^{-1}]

$\overline{\overline{\epsilon}}$ Permittivity tensor of the layer [Asm^{-1}V^{-1}]

ϵ_{t} Tangential component of the relative permittivity

ϵ_{n} Normal component of the relative permittivity

η_0 Free-space wave impedance [Ω]

θ Reflection phase [radian] (Chapter 3)

θ Incidence angle [radian] (Chapter 4.2)

κ Individual chiral coupling coefficient [sm^2]

$\widehat{\kappa}$ Effective chiral coupling coefficient [sm^2]

λ_0 Free-space wavelength [m]

μ_0 Vacuum permeability [Vsm^{-1}A^{-1}]

$\overline{\overline{\mu}}$ Permeability tensor of the layer [Vsm^{-1}A^{-1}]

μ_{t} Tangential component of the relative permeability

μ_{n} Normal component of the relative permeability

ϕ Reflection phase [radian]

χ Individual Tellegen coupling coefficient [sm^2]

$\widehat{\chi}$ Effective Tellegen coupling coefficient [sm^2]

Ω Individual omega coupling coefficient [sm^2]

$\widehat{\Omega}$ Effective omega coupling coefficient [sm^2]

ω Angular frequency [s^{-1}]

1. Introduction

In our everyday life, we observe different kinds of wave propagation phenomena, including mechanical and electromagnetic waves. These wave propagation scenarios involve interactions between waves and different materials. Depending on the structure of a medium through which a wave propagates, the wave-matter interaction can result in exciting effects. Amazing color distributions in feathers of a peacock or a butterfly, or iridescent colors on a jewel beetle's body are examples of the structural colors in nature which happen due to light interaction with regular and irregular nanostructural arrays on their bodies [1]. As another interesting effect of light-matter interaction, we can mention the light bending phenomenon which may have been known ever since humans started fishing. Properly controlling the wave-matter interaction, one can desirably manipulate the propagation of electromagnetic waves through a medium. The constitutive parameters of a material bulk, namely, the electric permittivity and magnetic permeability, are the key parameters in defining the electromagnetic response of a material. In order to tailor electromagnetic waves in some special ways, we may need to have materials with constitutive parameters which are not readily available in nature. One can utilize subwavelength arrangement of structural natural elements so as to artificially obtain unprecedented material properties. These artificial materials have been given the name "metamaterials".

Planar versions of metamaterials are called metasurfaces which are composed of two-dimensional (2D) arrays of polarizable inclusions enabling unprecedented manipulation of electromagnetic waves. The main research field in this thesis deals with designing functional metasurfaces. The first research direction of the thesis belongs to the general theory of off-band-transparent (OBT) symmetric and asymmetric absorbing metasurfaces. First, we introduce the concept of symmetric absorbing meta-

surfaces which absorb electromagnetic waves hitting any of their sides. As an example of symmetric absorbing metasurfaces, a novel OBT light absorber based on a single array of core-shell particles is introduced. In the second part of the study, we present the general theory of asymmetric absorbing metasurfaces. These metasurfaces absorb electromagnetic waves hitting one of their sides while offering different controllable properties for waves illuminating their other side. Chapter 2 and publications [I] and [II] present and discuss the results that are related to the concept of symmetric and asymmetric OBT absorbing metasurfaces.

The second research direction of the thesis is the general theory of OBT reflecting metasurfaces. Both symmetric and asymmetric reflecting metasurfaces are considered. We introduce metasurfaces which fully reflect electromagnetic waves hitting any of their sides while enabling independently controllable reflection phases from their different sides. Chapter 3 and publication [III] present and discuss the results that are related to the concept of symmetric and asymmetric OBT reflecting metasurfaces.

The third research direction of the thesis focuses on the general theory of Huygens' metasurfaces. We introduce metasurfaces which are transparent for waves hitting one of their sides while their behaviour for waves hitting their non-transparent side can be engineered in a controllable fashion. Furthermore, we introduce the concept of angularly independent Huygens' metasurfaces. Required design parameters for all-angle Huygens' metasurfaces are derived and possible designs for such metasurfaces are discussed. Chapter 4 and publications [IV] and [V] present and discuss the results that are related to the concept of Huygens' metasurfaces.

As the last main research direction of the thesis, we introduce a new method based on parity-time-symmetric ($\mathcal{PT}$-symmetric) systems to teleport plane waves behind highly reflective metallic screens. Chapter 5 and publication [VI] present and discuss the results that are related to the study of $\mathcal{PT}$-symmetric-based one-dimensional cloaking structures.

1.1 From metamaterials to metasurfaces

Recent introduction of a new class of artificial materials, so-called metamaterials, has opened new avenues with opportunities to create new materials with electromagnetic properties which are not readily available in nature. Metamaterial is an effectively homogenizable arrangement of ar-

tificial structural elements, designed to achieve advantageous and exotic electromagnetic properties [2–5]. In fact, the history of metamaterials may date back as far as the Lycurgus cup from the 4th AD that uses metallic nanoparticles colloids embedded in glass to dramatically change its color as a function of the illumination angle. However, the modern development in this area started in the mid-1990s. Extreme control of electromagnetic fields has become possible thanks to metamaterials leading to various research directions, applications, and a significant number of otherwise impossible devices such as perfect lenses and invisibility cloaks [2–4, 6–11].

To manipulate an electromagnetic wave so as to obtain a required wavefront, one needs to engineer the phase, amplitude, and polarization of the wave. In conventional electromagnetic and optical components this is obtained by propagating the electromagnetic wave through a bulk material over a distance which is usually much larger than the wavelength of the electromagnetic wave. This way the required changes in the properties of the wave are gradually accumulated along the optical path. The same scenario holds for the three-dimensional (3D) metamaterials, e.g., in transformation optics, we engineer a medium to tailor an electromagnetic wave in an unprecedented way [12, 13].

Although bulk metamaterials have proven successful in providing exotic electromagnetic effects, they suffer from considerable losses that are inherent to resonant elements typically used in their building blocks. There are also engineering challenges regarding manufacturing metamaterials, particularly in the visible range, which have yet to be dealt with [14, 15].

The main question which we face here is: How can we decrease the amount of losses and manufacturing difficulties in 3D metamaterial designs? As it was mentioned above, manipulating wavefronts utilizing 3D metamaterials rely on the propagation of waves over a distance in these artificial materials in order to accumulate required changes in phase, amplitude, and polarization. This begs the question: Can we utilize a different metamaterial design, e.g., low-profile 2D designs instead of 3D bulk structures, to get unprecedented control over electromagnetic waves? The previous question is tantamount to asking if it is possible to get the required changes in phase, amplitude, and polarization abruptly without having to propagate the electromagnetic waves through a lossy 3D metamaterial? Such a 2D version of metamaterials would enable tailoring electromagnetic wavefronts on either of its sides in unconventional ways.

These 2D metamaterials could incredibly resolve the problems related to manufacturing and losses which 3D metamaterials are facing.

To address these questions let us first briefly review relevant equivalence theorems of electromagnetics. Huygens' principle states that each element of any wavefront acts as a new source of disturbance, sending out secondary waves, and these secondary waves combine to form the new wavefront [16, 17]. A more rigorous formulation of this principle was presented by Love specifying the secondary sources in terms of balanced fictitious electric and magnetic currents [18]. Later on, this principle was generalized by Schelkunoff, today known as the surface equivalence principle, for non-zero field distributions on either side of a surface [19]. For these fields to exist on different sides of the imaginary layer, boundary conditions should be satisfied at the place of discontinuity. Boundary conditions dictate that to get such field distributions, equivalent electric and magnetic currents should be present on this imaginary layer. Therefore, according to the surface equivalence principle, for a given illumination, to create required field distributions on any side of the imaginary layer, we need to introduce both electric and magnetic currents in the layer. Required electric and magnetic currents can be engineered by passive and/or active elements. One can put electrically and magnetically polarizable inclusions in the layer to provide the required currents. However for some special field distributions, one needs to utilize active elements, i.e., current sources in the layer. Therefore, utilizing surface equivalence principle, we can design ultimately thin electrically and magnetically polarizable layers capable of tailoring field distributions in unprecedented ways. It should be noted that although metasurfaces enable manipulation of electromagnetic waves on any of their sides, these layers are not capable of creating any arbitrary field distributions.

Recently, metasurfaces, as the 2D version of bulk metamaterials have been utilized to provide the electric and magnetic currents required to produce the desirable electromagnetic fields distributions in response to a given input electromagnetic wave [20, 21]. Metasurfaces are 2D arrays of subwavelength electrically and magnetically polarizable unit cells with subwavelength thickness which provide unprecedented control of electromagnetic wavefronts. These surface versions of metamaterials enable moulding a given wavefront into a desired one by introducing spatial variations in the electromagnetic characteristics of the unit cells. Metasurfaces basically are sources of tangential fields discontinuities which en-

able tailoring electromagnetic waves in different ways [22–28]. Although metasurfaces have just recently attracted a great deal of attention, the idea of manipulating electromagnetic waves utilizing electrically thin layers is not new. Arrays or meshes of electrically thin conducting wires are among the first examples of thin composite layers which were utilized to manipulate electromagnetic waves [29]. Depending on operating frequency, these grids can be fully reflective or transparent for impinging incident plane waves [30–32]. Frequency-selective surfaces are another type of electrically thin composite layers which have been long utilized to filter electromagnetic waves [33, 34]. These surfaces are usually made up of periodic arrays of inclusions (e.g., electric dipoles) or periodically perforated metal screens. While metasurfaces are composed of subwavelength unit cells, in most of frequency-selective surface designs the array period is comparable with the wavelength. These screens possess only electric response, however, in order to arbitrarily manipulate electromagnetic waves utilizing metasurfaces, both electric and magnetic responses must be present in the layer. Reflectarrays and transmitarray are other similar concepts to that of metasurfaces with the array period mostly comparable with the wavelength. These layers have been long utilized to enable desirable variation of phase of reflected and transmitted fields in order to control wavefronts [35, 36]. However it was recently shown that arrays of small inclusions can also fully reflect electromagnetic waves with any desired phase distribution [37]. This new mirror design based on array of polarizable inclusions offers new functionalities such as unprecedentedly short focal length, which are not possible to achieve by conventional reflectarrays [38]. Holographic sheets are another example of thin layers which have been utilized to manipulate electromagnetic waves. Holographic layers are modulated impedance surfaces which employ holographic principle in order to control radiation from surface currents on metallic bodies [39–41]. However, most commonly, these screens possess only electric response.

Recently, two particular classes of metasurfaces, Huygens' metasurfaces and metamirrors, have been in the focus of metasurface research, receiving widespread attention day by day. Huygens' metasurfaces are reflectionless metasurfaces which are employed to tailor transmitted electromagnetic waves through them [42–47]. Metamirrors fully reflect incident electromagnetic waves tailoring reflected wavefronts at will [37, 38, 48–52].

There are some drawbacks with the recently reported studies on metasurfaces:

- Most of the reported studies on Huygens' metasurfaces consider symmetric structures meaning that they manipulate waves hitting their different sides in the same way. However, it is of great interest to design Huygens' metasurfaces which are capable of independently tailoring incident waves illuminating their different sides.

- Most of the proposed absorbing/reflecting metasurfaces are metal-backed structures. This feature is the source of two important problems with these metasurfaces. First, such metasurfaces interact with electromagnetic waves at all practical frequencies. However, it is of interest to design OBT absorbing/reflecting metasurfaces which allow off-band electromagnetic waves to pass through the structure. Second, it is not possible to engineer the behaviour of these metal-backed metasurfaces for waves hitting their other sides (unless we increase the number of the layers in the metasurfaces).

Throughout the thesis, we will address these two issues by designing symmetric and asymmetric OBT metasurfaces composed of single arrays of inclusions.

- All of the recently reported Huygens' metasurfaces are angularly-sensitive. This means that these metasurfaces work as Huygens' sheets for plane waves with one specific angle of incidence and as soon as the incidence angle deviates from the designed value, reflections from the metasurface appear.

To address this issue, we will present the general theory of all-angle Huygens' metasurfaces. In addition to addressing these issues, we will study a new metasurface based on $\mathcal{PT}$-symmetric systems. This study can open new avenues in designing functional metasurfaces.

1.2 Homogenization of metasurfaces

In order to analyse the operation of 2D metamaterials and design metasurfaces exhibiting new functionalities, an accurate and complete model

being capable of efficiently describing the physics behind them is required. Since metasurfaces are composed of 2D arrays of subwavelength electrically and magnetically polarizable unit cells, it is possible to homogenize and model them with macroscopic physical quantities. Due to the increasing attention paid to bianisotropic metasurfaces, it would be quite appropriate to develop a homogenization method which is capable of describing general bianisotropic metasurfaces. It is known that, although the conventional effective medium approaches are applicable to 3D metamaterials, they do not provide meaningful effective material parameters for a metasurface, since the retrieved parameters will depend on the choice of the effective thickness of the metasurface [53, 54]. In order to efficiently model the electromagnetic response of metasurfaces for a given external illumination, surface effective parameters, e.g., electric and magnetic surface susceptibilities, have been employed. These effective parameters associate the averaged electromagnetic fields existing on both sides of the array surface to the surface electric and magnetic polarization currents induced due to the incident wave. Two different techniques have been utilized to determine these effective surface parameters. In the first method these parameters are analytically extracted from simulated or measured scattering parameters of an impinging wave on a metasurface [53, 55]. This approach is similar to the Nicolson–Ross–Weir method which is employed to model 3D metamaterials [56]. Despite the simplicity and accuracy of this method, it requires a new simulated or measured scattering parameters every time a lattice parameter changes. In the second method, the building blocks of metasurfaces are modelled as point electric and magnetic dipoles. In this model the effective surface parameters of a metasurface are analytically related to the scattering properties of each inclusion (i.e., individual polarizabilities) and lattice parameters describing interactions between the array inclusions [2, 20, 21, 57–63]. The main advantage of this algorithm is the ability of evaluation and re-extraction of the effective surface parameters when any of the lattice parameters changes, without any need for additional simulation or measurement. Throughout this thesis we utilize a similar method to the one introduced by Niemi et al. [57], since it proposes a model for a general bianisotropic layer. Here we briefly review this method, since it will be employed in most of the upcoming sections.

The electromagnetic response of a generic metasurface for a normally incident electromagnetic plane wave can be modelled utilizing the relations

between the induced electric dipole moments $\mathbf{p}$, magnetic dipole moments $\mathbf{m}$, and the local electromagnetic fields $\mathbf{E}_{\mathrm{loc}}$ and $\mathbf{H}_{\mathrm{loc}}$ at the position of the unit cells

$$\begin{bmatrix} \mathbf{p} \\ \mathbf{m} \end{bmatrix} = \begin{bmatrix} \overline{\overline{\alpha}}_{\mathrm{ee}} & \overline{\overline{\alpha}}_{\mathrm{em}} \\ \overline{\overline{\alpha}}_{\mathrm{me}} & \overline{\overline{\alpha}}_{\mathrm{mm}} \end{bmatrix} \cdot \begin{bmatrix} \mathbf{E}_{\mathrm{loc}} \\ \mathbf{H}_{\mathrm{loc}} \end{bmatrix}. \tag{1.1}$$

Here, polarizabilities of individual particles, denoted as $\overline{\overline{\alpha}}_{\mathrm{ij}}$, define the response of a single particle in free space to the incident electromagnetic fields. There are two key points to be considered. First, since we consider an array of densely located polarizable subwavelength unit cells, inter-unit-cells interactions may play a significant role in the overall electromagnetic response of the metasurface. Second, the array period and thickness are much smaller than the free-space wavelength, so higher order modes do not contribute to the radiated plane-wave fields of the infinite array and we do not need to consider them. The local fields can be modelled as the sums of the external incident field and the interaction field caused by the induced dipole moments in other cells:

$$\begin{aligned} \mathbf{E}_{\mathrm{loc}} &= \mathbf{E}_{\mathrm{inc}} + \overline{\overline{\beta}}_{\mathrm{e}} \cdot \mathbf{p}, \\ \mathbf{H}_{\mathrm{loc}} &= \mathbf{H}_{\mathrm{inc}} + \overline{\overline{\beta}}_{\mathrm{m}} \cdot \mathbf{m}, \end{aligned} \tag{1.2}$$

where the explicit formulations for the interaction constants tensors $\overline{\overline{\beta}}_{\mathrm{e}}$ and $\overline{\overline{\beta}}_{\mathrm{m}}$ read [2]:

$$\begin{gathered} \overline{\overline{\beta}}_{\mathrm{e}} = \left[\mathrm{Re}\left\{ -\frac{jk_0}{4\epsilon_0 S}\left(1 - \frac{1}{jk_0\rho}\right) e^{-jk_0\rho} \right\} + j\left(\frac{k_0^3}{6\pi\epsilon_0} - \frac{k_0}{2\epsilon_0 S} \right) \right] \overline{\overline{I}}_{\mathrm{t}}, \\ \overline{\overline{\beta}}_{\mathrm{m}} = \frac{\overline{\overline{\beta}}_{\mathrm{e}}}{\eta_0^2}, \qquad \rho = \frac{\sqrt{S}}{1.438}, \end{gathered} \tag{1.3}$$

in which k_0, S, and η_0 are the free-space wavenumber, the unit cell area, and the free-space wave impedance, respectively. As a result, the induced electric and magnetic moments in a metasurface can be rewritten in terms of effective polarizbilities and the incident electromagnetic fields

$$\begin{bmatrix} \mathbf{p} \\ \mathbf{m} \end{bmatrix} = \begin{bmatrix} \overline{\overline{\widehat{\alpha}}}_{\mathrm{ee}} & \overline{\overline{\widehat{\alpha}}}_{\mathrm{em}} \\ \overline{\overline{\widehat{\alpha}}}_{\mathrm{me}} & \overline{\overline{\widehat{\alpha}}}_{\mathrm{mm}} \end{bmatrix} \cdot \begin{bmatrix} \mathbf{E}_{\mathrm{inc}} \\ \mathbf{H}_{\mathrm{inc}} \end{bmatrix}. \tag{1.4}$$

Explicit formulas for the effective polarizabilities in terms of the individual polarizabilities and interaction constants can be found in [57].

Throughout chapters 2, 3, and section 4.1, we study metasurfaces under normally incident plane waves and concentrate on uniaxial metasurfaces, isotropic in the plane of the layer. Hereafter, we will distinguish between illuminations of the metasurface from its two opposite sides, along $-\mathbf{z}_0$

and $\mathbf{z}_0$ ($\mathbf{z}_0$ is the unit vector normal to the metasurface). For these two cases, $(+/-)$ signs will be used where the top and bottom signs correspond to the incident plane waves propagating in $-\mathbf{z}_0$ and $\mathbf{z}_0$ directions, respectively. The uniaxial symmetry allows only isotopic response and rotation around the axis $\mathbf{z}_0$. Thus, all the polarizabilities in (1.4) take the forms:

$$\begin{aligned} \overline{\overline{\widehat{\alpha}}}_{\mathrm{ee}} &= \widehat{\alpha}_{\mathrm{ee}}^{\mathrm{co}}\overline{\overline{I}}_{\mathrm{t}} + \widehat{\alpha}_{\mathrm{ee}}^{\mathrm{cr}}\overline{\overline{J}}_{\mathrm{t}}, \qquad & \overline{\overline{\widehat{\alpha}}}_{\mathrm{mm}} &= \widehat{\alpha}_{\mathrm{mm}}^{\mathrm{co}}\overline{\overline{I}}_{\mathrm{t}} + \widehat{\alpha}_{\mathrm{mm}}^{\mathrm{cr}}\overline{\overline{J}}_{\mathrm{t}}, \\ \overline{\overline{\widehat{\alpha}}}_{\mathrm{em}} &= \widehat{\alpha}_{\mathrm{em}}^{\mathrm{co}}\overline{\overline{I}}_{\mathrm{t}} + \widehat{\alpha}_{\mathrm{em}}^{\mathrm{cr}}\overline{\overline{J}}_{\mathrm{t}}, \qquad & \overline{\overline{\widehat{\alpha}}}_{\mathrm{me}} &= \widehat{\alpha}_{\mathrm{me}}^{\mathrm{co}}\overline{\overline{I}}_{\mathrm{t}} + \widehat{\alpha}_{\mathrm{me}}^{\mathrm{cr}}\overline{\overline{J}}_{\mathrm{t}}, \end{aligned} \tag{1.5}$$

where indices 'co' and 'cr' refer to the symmetric and anti-symmetric parts of the corresponding dyadics, respectively. Here, $\overline{\overline{I}}_{\mathrm{t}} = \overline{\overline{I}} - \mathbf{z}_0\mathbf{z}_0$ is the 2D unit dyadic, and $\overline{\overline{J}}_{\mathrm{t}} = \mathbf{z}_0 \times \overline{\overline{I}}_{\mathrm{t}}$ is the vector-product operator. In the Cartesian coordinate system the corresponding matrix forms read

$$\overline{\overline{I}}_{\mathrm{t}} : \begin{bmatrix} 1 & 0 \\ 0 & 1 \end{bmatrix}, \quad \overline{\overline{J}}_{\mathrm{t}} : \begin{bmatrix} 0 & -1 \\ 1 & 0 \end{bmatrix}. \tag{1.6}$$

In the following sections, effects of different classes of electromagnetic couplings present in bianisotropic metasurfaces will be studied, so in the last set of relations, it is convenient to separate the coupling coefficients responsible for reciprocal and non-reciprocal coupling processes:

$$\begin{aligned} \overline{\overline{\widehat{\alpha}}}_{\mathrm{em}} &= (\widehat{\chi} + j\widehat{\kappa})\overline{\overline{I}}_{\mathrm{t}} + (\widehat{V} + j\widehat{\Omega})\overline{\overline{J}}_{\mathrm{t}}, \\ \overline{\overline{\widehat{\alpha}}}_{\mathrm{me}} &= (\widehat{\chi} - j\widehat{\kappa})\overline{\overline{I}}_{\mathrm{t}} + (-\widehat{V} + j\widehat{\Omega})\overline{\overline{J}}_{\mathrm{t}}. \end{aligned} \tag{1.7}$$

Here comes the classification of magnetoelectric coupling effects in terms of reciprocity and the symmetry of their magnetoelectric coupling dyadics. There are certain restrictions imposed by reciprocity on the polarizabilities:

$$\overline{\overline{\widehat{\alpha}}}_{\mathrm{em}} = -\overline{\overline{\widehat{\alpha}}}_{\mathrm{me}}^{\mathrm{T}}, \quad \overline{\overline{\widehat{\alpha}}}_{\mathrm{ee}} = \overline{\overline{\widehat{\alpha}}}_{\mathrm{ee}}^{\mathrm{T}}, \quad \overline{\overline{\widehat{\alpha}}}_{\mathrm{mm}} = \overline{\overline{\widehat{\alpha}}}_{\mathrm{mm}}^{\mathrm{T}}. \tag{1.8}$$

According to these conditions, there are two reciprocal classes (chiral $\widehat{\kappa}$ and omega $\widehat{\Omega}$) and two non-reciprocal classes ("moving" $\widehat{V}$ and Tellegen $\widehat{\chi}$) [64]. The four main types of magnetoelectric couplings are summarized in Table 1.1. Note also that for reciprocal particles the electric and magnetic polarizabilities $\overline{\overline{\widehat{\alpha}}}_{\mathrm{ee}}$ and $\overline{\overline{\widehat{\alpha}}}_{\mathrm{mm}}$ are always symmetric dyadics meaning that $\widehat{\alpha}_{\mathrm{ee}}^{\mathrm{cr}} = 0$ and $\widehat{\alpha}_{\mathrm{mm}}^{\mathrm{cr}} = 0$ [64].

For a normally impinging incident wave, the reflected and transmitted fields from a general bianisotropic metasurface read [57]

$$\begin{aligned} \mathbf{E}_{\mathrm{r}} = -\frac{j\omega}{2S}\Bigg\{ &\left[\eta_0\widehat{\alpha}_{\mathrm{ee}}^{\mathrm{co}} \pm \widehat{\alpha}_{\mathrm{em}}^{\mathrm{cr}} \pm \widehat{\alpha}_{\mathrm{me}}^{\mathrm{cr}} - \frac{1}{\eta_0}\widehat{\alpha}_{\mathrm{mm}}^{\mathrm{co}}\right]\overline{\overline{I}}_{\mathrm{t}} \\ &+ \left[\eta_0\widehat{\alpha}_{\mathrm{ee}}^{\mathrm{cr}} \mp \widehat{\alpha}_{\mathrm{em}}^{\mathrm{co}} \mp \widehat{\alpha}_{\mathrm{me}}^{\mathrm{co}} - \frac{1}{\eta_0}\widehat{\alpha}_{\mathrm{mm}}^{\mathrm{cr}}\right]\overline{\overline{J}}_{\mathrm{t}}\Bigg\} \cdot \mathbf{E}_{\mathrm{inc}} = \overline{\overline{R}}_{\mp\mathbf{z}_0} \cdot \mathbf{E}_{\mathrm{inc}}, \end{aligned} \tag{1.9}$$

Table 1.1. Magnetoelectric coupling effects (parameters Ω, κ, V and χ for lossless structures are real)

Basic types of magnetoelectric coupling effects			
Omega	Chiral	Moving	Tellegen
$\overline{\overline{\alpha}}_{\mathrm{em}} = \overline{\overline{\alpha}}_{\mathrm{me}} = j\Omega\overline{\overline{J}}_{\mathrm{t}}$	$\overline{\overline{\alpha}}_{\mathrm{em}} = -\overline{\overline{\alpha}}_{\mathrm{me}} = j\kappa\overline{\overline{I}}_{\mathrm{t}}$	$\overline{\overline{\alpha}}_{\mathrm{em}} = -\overline{\overline{\alpha}}_{\mathrm{me}} = V\overline{\overline{J}}_{\mathrm{t}}$	$\overline{\overline{\alpha}}_{\mathrm{em}} = \overline{\overline{\alpha}}_{\mathrm{me}} = \chi\overline{\overline{I}}_{\mathrm{t}}$

$$\begin{aligned}\mathbf{E}_{\mathrm{t}} = \Bigg\{ &\left[1 - \frac{j\omega}{2S}\left(\eta_0\widehat{\alpha}^{\mathrm{co}}_{\mathrm{ee}} \pm \widehat{\alpha}^{\mathrm{cr}}_{\mathrm{em}} \mp \widehat{\alpha}^{\mathrm{cr}}_{\mathrm{me}} + \frac{1}{\eta_0}\widehat{\alpha}^{\mathrm{co}}_{\mathrm{mm}}\right)\right]\overline{\overline{I}}_{\mathrm{t}} \\ &-\frac{j\omega}{2S}\left[\eta_0\widehat{\alpha}^{\mathrm{cr}}_{\mathrm{ee}} \mp \widehat{\alpha}^{\mathrm{co}}_{\mathrm{em}} \pm \widehat{\alpha}^{\mathrm{co}}_{\mathrm{me}} + \frac{1}{\eta_0}\widehat{\alpha}^{\mathrm{cr}}_{\mathrm{mm}}\right]\overline{\overline{J}}_{\mathrm{t}}\Bigg\} \cdot \mathbf{E}_{\mathrm{inc}} = \overline{\overline{T}}_{\mp\mathbf{z}_0} \cdot \mathbf{E}_{\mathrm{inc}},\end{aligned} \tag{1.10}$$

in which ω is the angular frequency. Now we are ready to study different bianisotropic metasurfaces possessing different functionalities.

2. Absorbing metasurfaces

We consider possible approaches to design metasurfaces which perfectly absorb normally incident electromagnetic plane waves. Although designing absorbers for electromagnetic waves has a long history, introduction of metasurfaces has provided a new perspective on the field and led to the development of alternative design techniques for electromagnetic absorbers. Recently a great deal of research has been conducted on designing absorbing metasurfaces [65,66], however to the best of our knowledge, only a very limited set of opportunities have been explored so far. It should be noted that all the polarization-insensitive absorbers, which have been proposed so far, absorb only waves hitting one of their sides or when the two sides are illuminated by two coherent waves [67–69].

Here we introduce the general theory of symmetric and asymmetric OBT absorbing metasurfaces composed of a single array of inclusions. First, we study symmetric absorbing metasurfaces. For a general symmetric absorbing metasurface, we investigate the required conditions for electromagnetic properties of its unit cells. Core-shell particles as a possible building block for symmetric absorbing metasurfaces are employed. Then we extend the study to asymmetric absorbing metasurfaces and consider the design possibilities offered by the particles of all four fundamental classes of bianisotropic inclusions: reciprocal chiral and omega particles and nonreciprocal Tellegen and moving particles.

2.1 Symmetric absorbing metasurfaces

In this section, we consider symmetric absorbing metasurfaces. The concept will later be extended to asymmetric absorbing metasurfaces to exploit more functionalities of these metasurfaces.

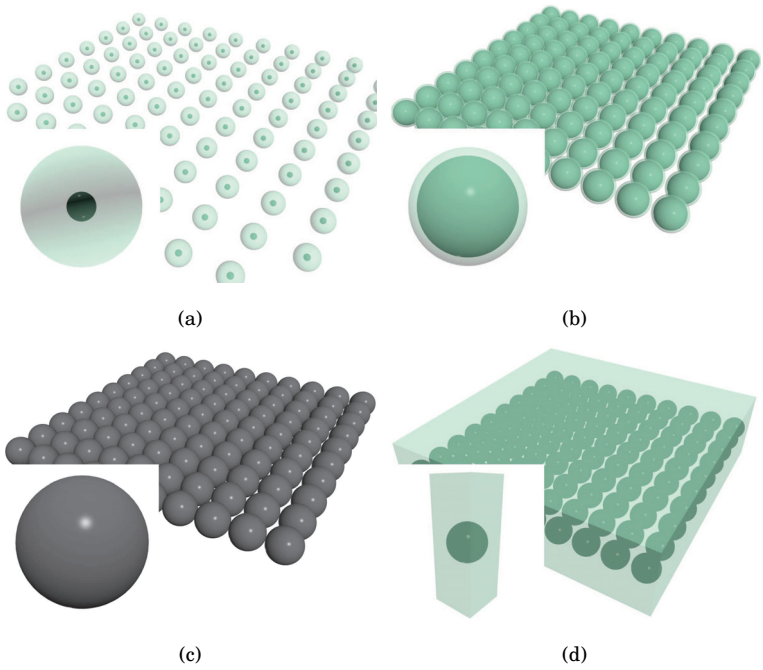

Figure 2.1. Geometry of the proposed designs for (a) Design A, (b) Design B, (c) Design C, and (d) Design D.

Let us think of a single array of particles which absorbs light[1] hitting either or both sides of it while being transparent for waves beyond the absorption frequency band. Before starting our analysis, it should be noted that in this section, in contrast to the other sections, the time dependence of the form $e^{-i\omega t}$ is assumed[2] (to be consistent with the time dependence assumption in publication [I]). Considering the new time dependence assumption, the reflected and transmitted fields from a general bianisotropic metasurface for a normally incident plane wave [see (1.9) and (1.10)] can be rewritten as:

$$\begin{aligned}\mathbf{E}_{\mathrm{r}} = \frac{i\omega}{2S}\Bigg\{&\left[\eta_0\widehat{\alpha}_{\mathrm{ee}}^{\mathrm{co}} \pm \widehat{\alpha}_{\mathrm{em}}^{\mathrm{cr}} \pm \widehat{\alpha}_{\mathrm{me}}^{\mathrm{cr}} - \frac{1}{\eta_0}\widehat{\alpha}_{\mathrm{mm}}^{\mathrm{co}}\right]\overline{\overline{I}}_{\mathrm{t}} \\ &+ \left[\eta_0\widehat{\alpha}_{\mathrm{ee}}^{\mathrm{cr}} \mp \widehat{\alpha}_{\mathrm{em}}^{\mathrm{co}} \mp \widehat{\alpha}_{\mathrm{me}}^{\mathrm{co}} - \frac{1}{\eta_0}\widehat{\alpha}_{\mathrm{mm}}^{\mathrm{cr}}\right]\overline{\overline{J}}_{\mathrm{t}}\Bigg\} \cdot \mathbf{E}_{\mathrm{inc}},\end{aligned} \tag{2.1}$$

$$\begin{aligned}\mathbf{E}_{\mathrm{t}} = \Bigg\{&\left[1 + \frac{i\omega}{2S}\left(\eta_0\widehat{\alpha}_{\mathrm{ee}}^{\mathrm{co}} \pm \widehat{\alpha}_{\mathrm{em}}^{\mathrm{cr}} \mp \widehat{\alpha}_{\mathrm{me}}^{\mathrm{cr}} + \frac{1}{\eta_0}\widehat{\alpha}_{\mathrm{mm}}^{\mathrm{co}}\right)\right]\overline{\overline{I}}_{\mathrm{t}} \\ &+ \frac{i\omega}{2S}\left[\eta_0\widehat{\alpha}_{\mathrm{ee}}^{\mathrm{cr}} \mp \widehat{\alpha}_{\mathrm{em}}^{\mathrm{co}} \pm \widehat{\alpha}_{\mathrm{me}}^{\mathrm{co}} + \frac{1}{\eta_0}\widehat{\alpha}_{\mathrm{mm}}^{\mathrm{cr}}\right]\overline{\overline{J}}_{\mathrm{t}}\Bigg\} \cdot \mathbf{E}_{\mathrm{inc}}.\end{aligned} \tag{2.2}$$

[1] In this section, we use the word "light" instead of "electromagnetic wave" to be consistent with publication [I].

[2] In all other parts of the thesis, the time dependence of the form $e^{j\omega t}$ is assumed.

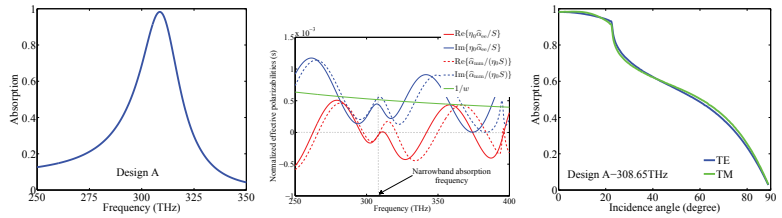

(a) (b) (c)

Figure 2.2. Design A [see Fig. 2.1(a)]: (a) Absorption as a function of the frequency. (b) Normalized effective electric and magnetic polarizabilities. (c) Absorption as a function of the incidence angle for 308.65 THz.

The definition of a perfect absorber implies that

$$\mathbf{E}_{\mathrm{r}} = 0, \quad \mathbf{E}_{\mathrm{t}} = 0. \tag{2.3}$$

In the case of symmetric absorption, both terms proportional to $\overline{\overline{I}}_{\mathrm{t}}$ and $\overline{\overline{J}}_{\mathrm{t}}$ in (2.1) and (2.2) must equal zero for both choices of the $\pm$ signs. This means that to have symmetric absorption, all the electromagnetic coupling coefficients must vanish:

$$\widehat{\alpha}_{\mathrm{em}}^{\mathrm{cr}} = \widehat{\alpha}_{\mathrm{me}}^{\mathrm{cr}} = \widehat{\alpha}_{\mathrm{em}}^{\mathrm{co}} = \widehat{\alpha}_{\mathrm{me}}^{\mathrm{co}} = 0. \tag{2.4}$$

This brings us to the conclusion that the only possible realization of symmetric total absorption is to utilize metasurfaces composed of inclusions which are both electrically and magnetically polarizable with balanced polarizabilities as in a Huygens' pair,

$$\frac{\eta_0}{S}\widehat{\alpha}_{\mathrm{ee}} = \frac{1}{\eta_0 S}\widehat{\alpha}_{\mathrm{mm}} = \frac{i}{\omega}, \tag{2.5}$$

with all the other polarizability components being zero. To design a metasurface it is more preferable to work with the polarizabilities of individual unit cells in free space instead of the effective polarizabilities. The corresponding individual polarizabilities read [57]

$$\eta_0\alpha_{\mathrm{ee}} = \frac{1}{\eta_0}\alpha_{\mathrm{mm}} = \left(\frac{\omega}{iS} + \frac{\beta_{\mathrm{e}}}{\eta_0}\right)^{-1}. \tag{2.6}$$

Many different designs can be utilized to provide the desired polarizabilities in (2.6). Recently, we presented an example of this kind of OBT symmetric absorbers for microwave frequencies [70]. Here, as another example, we design a new symmetric light absorber based on the theory developed in this section. We employ core-shell particles as the building blocks of symmetric absorbing metasurfaces. For an optically small isotropic core-shell sphere, the electric and magnetic polarizabilities read

$$\eta_0\alpha_{\mathrm{ee}} = \frac{6\pi c^2}{i\omega^3}a_1, \quad \frac{1}{\eta_0}\alpha_{\mathrm{mm}} = \frac{6\pi c^2}{i\omega^3}b_1. \tag{2.7}$$

Here a_1 and b_1 are the Mie coefficients (e.g., [71]) and c is the speed of light. To design an absorbing metasurface, we just need to equate these polarizabilities with the required ones in (2.6). This way, we can estimate the design parameters (i.e., the dimensions of the particles and the array period) and then optimize them utilizing a commercial electromagnetic software [72]. Now, we can start designing a resonant symmetric absorber. Figure 2.1(a) shows the geometry of the absorber (Design A) which is composed of inclusions with a silver core and an amorphous n-doped silicon shell. In this design the radius of the silver core, the thickness of the amorphous n-doped silicon shell, and the array period are $r_{\mathrm{Ag}} = 44$ nm, $t_{\mathrm{n-Si}} = 127$ nm, $d = 700$ nm, respectively. The simulated absorption spectrum in Fig. 2.2(a) shows that at the resonance frequency almost all energy of the normally incident wave gets absorbed in the layer. Figure 2.2(b) shows that at the resonance frequency the designed layer provides the required balanced effective electric and magnetic polarizabilities in (2.5). The designed metasurface is not an angularly-stable absorber and absorption drops when the incidence angle increases [see Fig. 2.2(c)].

2.1.1 Contributions of this thesis (summary of related publications)

Publication [I], following the theory presented in publication [II], presents four different designs for symmetric OBT absorbing metasurfaces. These designs include resonant, ultrabroadband, angularly selective, and all-angle absorbers. The basic design utilizes core-shell particles as possible building blocks which can provide the required balanced electric and magnetic responses in both narrowband and broadband regimes [see Figs. 2.1(a) and 2.1(b)]. However, it is also shown that, for some specific design requirements, an array of silver particles are enough to fully absorb incident waves [see Figs. 2.1(c)]. This is so because in this layer, silver particles are designed so as to provide the required balanced electric and magnetic responses without any need for covering them by n-doped amorphous silicon shells. We proposed another design which is of more practical importance [see Figs. 2.1(d)]. In this design, instead of covering silver spheres with the n-doped amorphous silicon shells an array of silver spheres are put inside an n-doped amorphous silicon slab. The physics behind each design is explained and accompanied by numerical simulations.

2.2 Asymmetric absorbing metasurfaces

Now let us analyse the case for which a metasurface fully absorbs electromagnetic waves illuminating one of its sides and try to explore all different functionalities that can be achieved for waves hitting the other side of the metasurface. Satisfying the absorption condition in (1.9) and (1.10) for waves hitting one of the two sides of the metasurface corresponds to conditions

$$\begin{aligned}
\eta_0\widehat{\alpha}_{\rm ee}^{\rm co}-\frac{1}{\eta_0}\widehat{\alpha}_{\rm mm}^{\rm co}&=\mp(\widehat{\alpha}_{\rm em}^{\rm cr}+\widehat{\alpha}_{\rm me}^{\rm cr}),\\
\eta_0\widehat{\alpha}_{\rm ee}^{\rm cr}-\frac{1}{\eta_0}\widehat{\alpha}_{\rm mm}^{\rm cr}&=\pm(\widehat{\alpha}_{\rm em}^{\rm co}+\widehat{\alpha}_{\rm me}^{\rm co}),\\
\eta_0\widehat{\alpha}_{\rm ee}^{\rm co}+\frac{1}{\eta_0}\widehat{\alpha}_{\rm mm}^{\rm co}&=\frac{2S}{j\omega}\mp(\widehat{\alpha}_{\rm em}^{\rm cr}-\widehat{\alpha}_{\rm me}^{\rm cr}),\\
\eta_0\widehat{\alpha}_{\rm ee}^{\rm cr}+\frac{1}{\eta_0}\widehat{\alpha}_{\rm mm}^{\rm cr}&=\pm(\widehat{\alpha}_{\rm em}^{\rm co}-\widehat{\alpha}_{\rm me}^{\rm co}).
\end{aligned}\tag{2.8}$$

Here the upper signs correspond to $-\mathbf{z}_0$-directed and the lower signs to the $\mathbf{z}_0$-directed incident plane waves. Using the same conditions for total absorption for the opposite incidence direction in (1.9) and (1.10), we find the reflected and transmitted electric fields when the incidence is from the other side:

$$\begin{aligned}
\mathbf{E}_{\rm r}&=\frac{j\omega}{S}\left\{\pm[\widehat{\alpha}_{\rm em}^{\rm cr}+\widehat{\alpha}_{\rm me}^{\rm cr}]\,\overline{\overline{I}}_{\rm t}\mp[\widehat{\alpha}_{\rm em}^{\rm co}+\widehat{\alpha}_{\rm me}^{\rm co}]\,\overline{\overline{J}}_{\rm t}\right\}\cdot\mathbf{E}_{\rm inc},\\
\mathbf{E}_{\rm t}&=\frac{j\omega}{S}\left\{\pm[\widehat{\alpha}_{\rm em}^{\rm cr}-\widehat{\alpha}_{\rm me}^{\rm cr}]\,\overline{\overline{I}}_{\rm t}\mp[\widehat{\alpha}_{\rm em}^{\rm co}-\widehat{\alpha}_{\rm me}^{\rm co}]\,\overline{\overline{J}}_{\rm t}\right\}\cdot\mathbf{E}_{\rm inc}.
\end{aligned}\tag{2.9}$$

It is seen from these equations that setting a bianisotropic metasurface to work as an absorber from one side, it is possible to realize some special properties (in reflection and transmission) for the waves illuminating the other side of the metasurface. Let us start with reciprocal metasurfaces. Due to the reciprocity, there are no cross components for electric and magnetic polarizabilities, $\widehat{\alpha}_{\rm ee}^{\rm cr}=0$, $\widehat{\alpha}_{\rm mm}^{\rm cr}=0$, and the coupling polarizabilities satisfy

$$\widehat{\alpha}_{\rm em}^{\rm co}=-\widehat{\alpha}_{\rm me}^{\rm co},\qquad\widehat{\alpha}_{\rm em}^{\rm cr}=\widehat{\alpha}_{\rm me}^{\rm cr}.\tag{2.10}$$

According to (1.7), here, the co- and cross-components of the coupling dyadic correspond to chiral and omega couplings [64], respectively. Considering the polarizability conditions for a chiral metasurface and requirements for a one-way absorbing metasurface in (2.9), it becomes clear that there is no possibility to design a one-way absorbing metasurface possessing chiral coupling while being able to engineer the transmission from the other side of the metasurface. Therefore to design a reciprocal absorbing metasurface there should be no chirality in the structure of the

absorber [70]. In 1980s, a new class of absorbing layers based on metal-backed chiral slabs was introduced which may look contradictory to our last statement [73–75]. However, later it was both theoretically and experimentally shown that chirality is not essential to create fully absorbing layers [76–78]. In addition to this, it should be noted that an absorber composed of a metal-backed chiral slab is effectively a non-chiral structure due to the presence of the metallic mirror behind the chiral slab.

Now let us consider a metasuface possessing omega coupling. It is seen from (2.9) that an omega metasurface may enable one-way absorption while providing control over the co-polarized reflection for waves illuminating the other side of the layer. Considering the polarizability conditions for an omega metasurface and requirements for a one-way absorbing metasurface in (2.8), we notice that in contrast to the chiral metasurface, in this case the omega coupling coefficient $\widehat{\alpha}_{\mathrm{me}}^{\mathrm{cr}}$ is not fixed by the conditions for one-way absorption. The required polarizabilities for such a metasurface read

$$\widehat{\alpha}_{\mathrm{ee}}^{\mathrm{co}} = \frac{S}{j\omega\eta_0} \mp \frac{1}{\eta_0}\widehat{\alpha}_{\mathrm{me}}^{\mathrm{cr}}, \qquad \widehat{\alpha}_{\mathrm{mm}}^{\mathrm{co}} = \frac{\eta_0 S}{j\omega} \pm \eta_0\widehat{\alpha}_{\mathrm{me}}^{\mathrm{cr}}. \tag{2.11}$$

There is an important point to be mentioned here. Omega coupling serves as a degree of freedom relaxing requirements on the electric and magnetic polarizabilities. This means that introducing omega coupling to a metasurface makes it possible to design an omega metasurface with a magnetic polarizability much smaller than the electric one. The reflected electric field from the non-absorbing side of the metasurface reads

$$\mathbf{E}_{\mathrm{r}} = \pm\frac{2j\omega}{S}\widehat{\alpha}_{\mathrm{em}}^{\mathrm{cr}}\overline{\overline{I}}_{\mathrm{t}} \cdot \mathbf{E}_{\mathrm{inc}}. \tag{2.12}$$

Therefore, we can engineer an omega metasurface so as to control the co-polarized reflection from the opposite side of the sheet, while maintaining the matching and total absorption properties of the absorbing side. Basically, most of the metal-backed absorbing metasurfaces fall into this category of asymmetric absorbers. However, as it was mentioned before, these metal-backed absorbers block the electromagnetic waves at all practical frequencies and have fixed properties (reflection coefficient equals -1) for the non-absorbing side. An example of omega absorbing metasurfaces which utilizes no ground plane was recently presented in [79].

Allowing non-reciprocity in metasurfaces enables more otherwise impossible functionalities. Let us consider two non-reciprocal Tellegen and "moving" metasurfaces. For these cases, the electromagnetic coupling co-

efficients satisfy

$$\widehat{\alpha}_{\rm em}^{\rm co}=\widehat{\alpha}_{\rm me}^{\rm co},\qquad \widehat{\alpha}_{\rm em}^{\rm cr}=-\widehat{\alpha}_{\rm me}^{\rm cr}, \tag{2.13}$$

corresponding to Tellegen and moving cases, respectively [64]. As it can be seen from (2.9), a Tellegen metasurface can serve as a perfect absorber from one of its sides while enabling control over cross-polarized reflection for waves illuminating its non-absorbing side. Substituting polarizability conditions for a Tellegen metasurface in (2.8), the required polarizabilities for a one-way absorbing Tellegen metasurface read

$$\eta_0\widehat{\alpha}_{\rm ee}^{\rm co}=\frac{1}{\eta_0}\widehat{\alpha}_{\rm mm}^{\rm co}=\frac{S}{j\omega},\quad \eta_0\widehat{\alpha}_{\rm ee}^{\rm cr}=\pm\widehat{\alpha}_{\rm em}^{\rm co}=-\frac{1}{\eta_0}\widehat{\alpha}_{\rm mm}^{\rm cr}. \tag{2.14}$$

Thus, the effect of Tellegen coupling should be balanced with the nonreciprocity in both electric and magnetic polarizabilities. The reflected electric field from the non-absorbing side of the metasurface reads

$$\mathbf{E}_{\rm r}=\mp\frac{2j\omega}{S}\widehat{\alpha}_{\rm em}^{\rm co}\overline{\overline{J}}_{\rm t}\cdot\mathbf{E}_{\rm inc}. \tag{2.15}$$

Therefore, a Tellegen metasurface can serve as a perfect absorber from one side and a twist polarizer in reflection from the other side. Utilizing a moving metasurface, one can design a one-way absorber while getting control over the co-polarized transmission for incident waves in the opposite direction [see (2.9)]. The required polarizabilities to design a one-way absorbing metasurface, possessing moving coupling, can be derived from (2.8):

$$\eta_0\widehat{\alpha}_{\rm ee}^{\rm co}=\frac{1}{\eta_0}\widehat{\alpha}_{\rm mm}^{\rm co}=\frac{S}{j\omega}\mp\widehat{\alpha}_{\rm em}^{\rm cr},\quad \widehat{\alpha}_{\rm ee}^{\rm cr}=\widehat{\alpha}_{\rm ee}^{\rm cr}=0. \tag{2.16}$$

The transmitted electric field from the opposite side reads (for nonreciprocal sheets the transmission coefficient is not anymore necessarily symmetric):

$$\mathbf{E}_{\rm t}=\pm\frac{2j\omega}{S}\widehat{\alpha}_{\rm em}^{\rm cr}\overline{\overline{I}}_{\rm t}\cdot\mathbf{E}_{\rm inc}. \tag{2.17}$$

It becomes even more interesting if we try to make the transmission equal to unity which happens for $\widehat{\alpha}_{\rm em}^{\rm cr}=\pm S/(2j\omega)$. For this case the required conditions in (2.16) can be rewritten as

$$\eta_0\widehat{\alpha}_{\rm ee}^{\rm co}=\pm\widehat{\alpha}_{\rm em}^{\rm cr}=\frac{1}{\eta_0}\widehat{\alpha}_{\rm mm}^{\rm co}=\frac{S}{j2\omega}. \tag{2.18}$$

This is an interesting result showing that all the polarizabilities are balanced. We can conclude that this interesting structure has the property of the ultimately thin (a single layer of dipole particles) isolator: from one side it acts as a total absorber while from the other side, the sheet is transparent.

2.2.1 Contributions of this thesis (summary of related publications)

Publication [II] presents the general theory of electromagnetic waves absorption in single arrays of electrically small particles. We start with the concept of single arrays of resonant electrically and magnetically polarizable particles which absorb electromagnetic waves hitting any of their sides (symmetric absorption) while being transparent for waves at other frequencies. Then, introducing different classes of bianisotropic couplings in the unit cells, we exploit all the possibilities and limitations in realizing OBT asymmetric absorbing metasurfaces in ultimately thin layers.

3. Reflecting metasurfaces (Metamirrors)

When we think of electromagnetic wave mirrors, the simplest mirror which comes to mind is a metallic sheet working as a nearly perfect mirror for microwave frequencies (reflection coefficient $R = -1$). Artificial magnetic walls are other examples of electromagnetic wave mirrors which can fully reflect electromagnetic waves without reversing their phase [80] ($R = +1$). To violate the simple law of reflection, we need mirrors with arbitrarily engineered surface reflection phase distribution. Reflectarrays, enabling mirrors with general control over the reflection phase, have been utilized to tailor the reflected waves at will [35]. A common issue with most of these mirrors is that they are metal-backed structures, making them detectable for electromagnetic waves at all practical frequencies. However, for some applications such as optically transparent microwave reflectarrays or frequency-selective reflectors, OBT mirrors are of great interest. Furthermore, we can think of an OBT mirror, fully reflecting electromagnetic waves hitting any of its sides, which offers different reflection phase distributions on its two faces. This feature is not attainable with conventional mirrors due to the presence of metallic sheets in their structures unless more layers are added to the design of the mirrors. In previous sections, we studied OBT absorbing metasurfaces composed of arrays of electrically and magnetically polarizable particles possibly possessing different classes of electromagnetic couplings. An interesting question one may ask at this point is whether it is possible to realize an OBT mirror composed of an array of electrically small polarizable inclusions resolving the issues with the conventional mirrors? Here, we present the concept of OBT metamirrors which offer possibilities for full control over the reflection phases of their different surfaces.

3.1 Symmetric metamirrors

Let us start with designing a symmetric mirror composed of an array of electrically small inclusions. Imagine a metamirror which symmetrically reflects waves hitting any of its sides. Reflection coefficients for such a metamirror can be written as

$$R_{-\mathbf{z}_0} = R_{+\mathbf{z}_0} = e^{j\phi}. \tag{3.1}$$

Demanding such reflection properties, the required effective polarizabilities can be written as [see (1.9) and (1.10)]

$$\eta_0 \widehat{\alpha}_{\mathrm{ee}}^{\mathrm{co}} = \frac{-2S}{\omega} e^{j\phi/2} \sin\left(\phi/2\right), \quad \frac{1}{\eta_0} \widehat{\alpha}_{\mathrm{mm}}^{\mathrm{co}} = \frac{2S}{j\omega} e^{j\phi/2} \cos\left(\phi/2\right), \tag{3.2}$$

with all the other polarizabilities being zero. Utilizing relations between the effective and individual polarizabilities [57], the individual polarizabilities related to these effective polarizabilities read

$$\eta_0 \alpha_{\mathrm{ee}}^{\mathrm{co}} = \frac{1 - e^{j\phi}}{1 - e^{j\phi} + j\frac{\omega\eta_0}{\beta_{\mathrm{e}} S}} \frac{\eta_0}{\beta_{\mathrm{e}}}, \quad \frac{1}{\eta_0} \alpha_{\mathrm{mm}}^{\mathrm{co}} = \frac{1 + e^{j\phi}}{1 + e^{j\phi} + j\frac{\omega\eta_0}{\beta_{\mathrm{e}} S}} \frac{\eta_0}{\beta_{\mathrm{e}}}. \tag{3.3}$$

As it can be seen from these conditions, for symmetric metamirrors, there should not be any electromagnetic coupling present, however, to provide any arbitrary reflection phase, both electric and magnetic responses should be present in the metasurfaces.

Let us now consider some known special cases of symmetric metamirrors. In (3.2), if we suppose $\phi = \pi$ (symmetric electric conductor) all the polarizabilities except the electric one become zero $\eta_0 \widehat{\alpha}_{\mathrm{ee}}^{\mathrm{co}} = 2S/j\omega$, as it is expected. For a symmetric magnetic wall, i.e., $\phi = 0$, only magnetic polarizability is non-zero $\widehat{\alpha}_{\mathrm{mm}}^{\mathrm{co}}/\eta_0 = 2S/j\omega$, as it should be. As examples of this kind of symmetric reflectors, we can mention symmetric magnetic walls presented in [81, 82] which are composed of arrays of single and double split-ring resonators.

3.2 Asymmetric metamirrors

In the previous section we considered symmetric metamirrors. Let us now think of a double-way OBT mirror composed of a single array of electrically small particles which provides different (independent) reflection phases for electromagnetic waves hitting its different sides. Such a mirror must provide the following reflection coefficients

$$R_{-\mathbf{z}_0} = e^{j\phi}, \quad R_{+\mathbf{z}_0} = e^{j\theta}. \tag{3.4}$$

The required effective polarizabilities for such a metamirror can be obtained by substituting these requirements in (1.9) and (1.10):

$$\begin{aligned}
\eta_0\widehat{\alpha}_{\mathrm{ee}}^{\mathrm{co}} &= \frac{S}{j\omega}\left[1-\frac{e^{j\phi}+e^{j\theta}}{2}\right],\\
\widehat{\alpha}_{\mathrm{em}}^{\mathrm{cr}} = \widehat{\alpha}_{\mathrm{me}}^{\mathrm{cr}} &= \frac{-S}{j\omega}\left[\frac{e^{j\phi}-e^{j\theta}}{2}\right],\\
\frac{1}{\eta_0}\widehat{\alpha}_{\mathrm{mm}}^{\mathrm{co}} &= \frac{S}{j\omega}\left[1+\frac{e^{j\phi}+e^{j\theta}}{2}\right].
\end{aligned} \tag{3.5}$$

These polarizabilities refer to an omega metasurface. This is physically understandable, because we demand this layer to show the same transmission properties but different co-polarized reflection properties for waves incident from the opposite directions.

Utilizing relations between effective and individual polarizabilities [57], the required individual polarizabilities of single inclusions can be written as

$$\begin{aligned}
\eta_0\alpha_{\mathrm{ee}}^{\mathrm{co}} &= \frac{1-e^{j(\theta+\phi)}+\frac{j\omega\eta_0}{\beta_{\mathrm{e}}S}\left[-\frac{1}{2}\left(e^{j\phi}+e^{j\theta}\right)+1\right]}{-e^{j(\theta+\phi)}+\left(1+j\frac{\omega\eta_0}{\beta_{\mathrm{e}}S}\right)^2}\frac{\eta_0}{\beta_{\mathrm{e}}},\\
\alpha_{\mathrm{em}}^{\mathrm{cr}} = \alpha_{\mathrm{me}}^{\mathrm{cr}} &= \frac{-\frac{j\omega\eta_0}{2\beta_{\mathrm{e}}S}\left(e^{j\phi}-e^{j\theta}\right)}{-e^{j(\theta+\phi)}+\left(1+j\frac{\omega\eta_0}{\beta_{\mathrm{e}}S}\right)^2}\frac{\eta_0}{\beta_{\mathrm{e}}},\\
\frac{1}{\eta_0}\alpha_{\mathrm{mm}}^{\mathrm{co}} &= \frac{1-e^{j(\theta+\phi)}+\frac{j\omega\eta_0}{\beta_{\mathrm{e}}S}\left[\frac{1}{2}\left(e^{j\phi}+e^{j\theta}\right)+1\right]}{-e^{j(\theta+\phi)}+\left(1+j\frac{\omega\eta_0}{\beta_{\mathrm{e}}S}\right)^2}\frac{\eta_0}{\beta_{\mathrm{e}}}.
\end{aligned} \tag{3.6}$$

These requirements for individual polarizabilities satisfy the necessary condition for lossless bianisotropic particles [83]

$$\begin{aligned}
&\mathrm{Im}\left\{\left(\overline{\overline{\alpha}}_{\mathrm{ee}}-\overline{\overline{\alpha}}_{\mathrm{em}}\cdot\overline{\overline{\alpha}}_{\mathrm{mm}}^{-1}\cdot\overline{\overline{\alpha}}_{\mathrm{me}}\right)^{-1}\right\} =\\
&\qquad\mathrm{Im}\left\{\beta_{\mathrm{e}}+\frac{j\omega\eta_0}{2S}\frac{e^{j\phi}+e^{j\theta}+2}{1-e^{j(\phi+\theta)}}\right\}\overline{\overline{I}}_{\mathrm{t}} = \frac{k_0^3}{6\pi\epsilon_0}\overline{\overline{I}}_{\mathrm{t}}.
\end{aligned} \tag{3.7}$$

Therefore, in order to design an asymmetric metamirror which fully reflects electromagnetic waves hitting any of its sides with independently different phases, we need to have an array of omega inclusions.

Up to now, we considered the case of uniform phase distributions over the surfaces of metamirrors. However, in most of applications it is of great interest to tailor the reflected waves from a metamirror. To this end, arbitrary surface reflection phase distribution should be engineered over the surfaces of a metamirror. Under the assumption of slow and smooth reflection phase variations along different surfaces of the metamirror, the physical optics approximation can be utilized to design each particle at any point on the metamirror [84]. Recently we proposed an OBT mirror based on the theory presented in this section [38].

3.2.1 Contributions of this thesis (summary of related publications)

Publication [III] presents the general theory of symmetric and asymmetric OBT metamirrors. We start with the simple case of symmetric mirrors composed of arrays of electrically small inclusions. It is shown that to get any arbitrary symmetric reflection phase, the unit cells must be both electrically and magnetically polarizable. Then, we generalize the theory and consider the case of asymmetric metamirrors. It is shown that in this case, in addition to being both electrically and magnetically polarizable, building blocks must possess bianisotropic omega coupling in order to get asymmetric and independent reflection phases for plane waves illuminating different sides of the metamirrors.

4. Huygens' metasurfaces

In recent years, there has been an increasing research interest in designing reflectionless metasurfaces known as Huygens' metasurfaces [42, 43, 46]. These layers are utilized in order to manipulate electromagnetic wavefronts in transmission while keeping the reflections as low as possible (ideally zero). A similar concept to that of the Huygens' metasurfaces is the concept of transmitarrays [36]. These conventional layers have been long utilized in radio and microwave communications to manipulate transmitted wavefronts. However, the array period in these layers is comparable with the wavelength of the incident wave.

Majority of studies on Huygens' metasurfaces propose symmetric transparent layers which tailor transmitted waves in the same way for incident waves hitting any of their sides. In the first part of this chapter, our main goal is to find out what functionalities are possible if one-way transparency is required. Can we make the layer fully reflecting or act as a twist polarizer or a phase shifter for plane waves coming from the non-transparent side?

In the second part of this chapter, we focus on the concept of angularly independent Huygens' metasurfaces. Despite the ever-increasing research effort devoted to the concept of Huygens' metasurfaces, there is a fundamental problem associated with most of these designs which greatly limits their functionalities. These metasurfaces can work as Huygens' metasurfaces for plane-wave incidences at only one incidence angle (usually the normal incidence is selected in designs). The main question which we are going to address is: Can we design an electrically thin polarization-independent all-angle reflectionless layer which is also capable of manipulating transmitted wavefronts? As to polarization-independent all-angle reflectionless response, the only known examples correspond to tunneling structures, namely, tunneling structures based on conjugate matched pair

of epsilon-negative and mu-negative slabs [85] and epsilon-negative layer coated with uniaxial layers [86]. However, in these multilayer structures the phase of the transmitted wave is the same as the phase of the incident wave. Another all-angle reflectionless structure based on $\mathcal{PT}$-symmetric systems was recently proposed which is composed of multilayer lossy slabs in front of an active layer [87]. However this design is polarization sensitive. Physical requirements in order to realize an all-angle passive absorber were studied in [88] where utilizing higher-order spatial dispersion effects was suggested as a possible route in order to realize such an all-angle reflectionless behaviour.

Here, we present the general concept of polarization-insensitive angularly independent lossless Huygens' metasurfaces. We determine the physical requirements on the surface parameters which ensure the desired response. Possible realizations for such metasurfaces are also investigated.

4.1 Transparent metasurfaces

Here, we study double-way (symmetric) and one-way (asymmetric) transparent metasurfaces. A one-way transparent metasurface is transparent for waves illuminating one of its sides, however, it enables manipulation of waves hitting the non-transparent side of the metasurface (i.e., engineered reflection and transmission). For such a metasurface the induced surface-averaged current densities must equal zero for illuminating the transparent side but have nontrivial and controllable values when illuminating the non-transparent side.

4.1.1 Symmetric transparent metasurfaces

Let us first consider the case of double-way transparent metasurfaces. For a general metasurface, with different classes of electromagnetic couplings, the reflected and transmitted plane waves due to a normal plane wave incidence can be written as [see (1.7), (1.9), and (1.10)]

$$\begin{aligned}\mathbf{E}_{\mathrm{r}} = -\frac{j\omega}{2S}\Bigg\{&\left[\eta_0\widehat{\alpha}_{\mathrm{ee}}^{\mathrm{co}} \pm 2j\widehat{\Omega} - \frac{1}{\eta_0}\widehat{\alpha}_{\mathrm{mm}}^{\mathrm{co}}\right]\overline{\overline{I}}_{\mathrm{t}} \\ &+ \left[\eta_0\widehat{\alpha}_{\mathrm{ee}}^{\mathrm{cr}} \mp 2\widehat{\chi} - \frac{1}{\eta_0}\widehat{\alpha}_{\mathrm{mm}}^{\mathrm{cr}}\right]\overline{\overline{J}}_{\mathrm{t}}\Bigg\}\cdot\mathbf{E}_{\mathrm{inc}},\end{aligned} \tag{4.1}$$

$$\begin{aligned}\mathbf{E}_{\mathrm{t}} = \Bigg\{&\left[1 - \frac{j\omega}{2S}\left(\eta_0\widehat{\alpha}_{\mathrm{ee}}^{\mathrm{co}} \pm 2\widehat{V} + \frac{1}{\eta_0}\widehat{\alpha}_{\mathrm{mm}}^{\mathrm{co}}\right)\right]\overline{\overline{I}}_{\mathrm{t}} \\ &- \frac{j\omega}{2S}\left[\eta_0\widehat{\alpha}_{\mathrm{ee}}^{\mathrm{cr}} \mp 2j\widehat{\kappa} + \frac{1}{\eta_0}\widehat{\alpha}_{\mathrm{mm}}^{\mathrm{cr}}\right]\overline{\overline{J}}_{\mathrm{t}}\Bigg\}\cdot\mathbf{E}_{\mathrm{inc}}.\end{aligned} \tag{4.2}$$

A transparent layer must not create any reflection and must not change the phase and amplitude of the incident wave when it passes through the metasurface:

$$\mathbf{E}_{\mathrm{r}} = 0, \qquad \mathbf{E}_{\mathrm{t}} = \mathbf{E}_{\mathrm{inc}}. \tag{4.3}$$

By applying these requirements in (4.1) and (4.2), we can obtain the necessary conditions for a transparent metasurface

$$\begin{aligned} \eta_0\widehat{\alpha}_{\mathrm{ee}}^{\mathrm{co}} \pm 2j\widehat{\Omega} - \frac{1}{\eta_0}\widehat{\alpha}_{\mathrm{mm}}^{\mathrm{co}} = 0, \qquad & \eta_0\widehat{\alpha}_{\mathrm{ee}}^{\mathrm{cr}} \mp 2\widehat{\chi} - \frac{1}{\eta_0}\widehat{\alpha}_{\mathrm{mm}}^{\mathrm{cr}} = 0, \\ \eta_0\widehat{\alpha}_{\mathrm{ee}}^{\mathrm{co}} \pm 2\widehat{V} + \frac{1}{\eta_0}\widehat{\alpha}_{\mathrm{mm}}^{\mathrm{co}} = 0, \qquad & \eta_0\widehat{\alpha}_{\mathrm{ee}}^{\mathrm{cr}} \mp 2j\widehat{\kappa} + \frac{1}{\eta_0}\widehat{\alpha}_{\mathrm{mm}}^{\mathrm{cr}} = 0. \end{aligned} \tag{4.4}$$

For a double-way transparent metasurface, we see from these conditions that all the polarizabilities must be zero, which is a trivial solution. However, this does not mean that the metasurface is simply absent. Zero dipole moments in each unit cell mean only that the surface-averaged electric and magnetic current densities are zero.

4.1.2 Asymmetric transparent metasurfaces

Let us now focus on the case of one-way transparent metasurfaces. To simplify the problem, let us think of a metasurface which is transparent for $+\mathrm{z}_0$-directed waves. The transparency conditions in (4.4) can be rewritten as

$$\begin{aligned} \eta_0\widehat{\alpha}_{\mathrm{ee}}^{\mathrm{co}} - \frac{1}{\eta_0}\widehat{\alpha}_{\mathrm{mm}}^{\mathrm{co}} = 2j\widehat{\Omega}, \qquad & \eta_0\widehat{\alpha}_{\mathrm{ee}}^{\mathrm{cr}} - \frac{1}{\eta_0}\widehat{\alpha}_{\mathrm{mm}}^{\mathrm{cr}} = -2\widehat{\chi}, \\ \eta_0\widehat{\alpha}_{\mathrm{ee}}^{\mathrm{co}} + \frac{1}{\eta_0}\widehat{\alpha}_{\mathrm{mm}}^{\mathrm{co}} = 2\widehat{V}, \qquad & \eta_0\widehat{\alpha}_{\mathrm{ee}}^{\mathrm{cr}} + \frac{1}{\eta_0}\widehat{\alpha}_{\mathrm{mm}}^{\mathrm{cr}} = -2j\widehat{\kappa}. \end{aligned} \tag{4.5}$$

The reflected and transmitted waves due to an incident plane wave hitting the non-transparent side of such a metasurface can be obtained by substituting conditions (4.5) in (4.1) and (4.2)

$$\mathbf{E}_{\mathrm{r}} = \frac{j2\omega}{S}\left(-j\widehat{\Omega}\overline{\overline{I}}_{\mathrm{t}} + \widehat{\chi}\overline{\overline{J}}_{\mathrm{t}}\right)\cdot\mathbf{E}_{\mathrm{inc}}, \quad \mathbf{E}_{\mathrm{t}} = \left[\left(1 - \frac{j2\omega}{S}\widehat{V}\right)\overline{\overline{I}}_{\mathrm{t}} - \frac{2\omega}{S}\widehat{\kappa}\overline{\overline{J}}_{\mathrm{t}}\right]\cdot\mathbf{E}_{\mathrm{inc}}. \tag{4.6}$$

Now, we are ready to exploit all the possibilities to design asymmetric transparent metasurfaces. Let us start with reciprocal metasurfaces. One-way transparency conditions in (4.5) show that there cannot be any chirality present in a one-way transparent metasurface, however, omega coupling may be allowed:

$$\eta_0\widehat{\alpha}_{\mathrm{ee}}^{\mathrm{co}} = j\widehat{\Omega} = -\frac{1}{\eta_0}\widehat{\alpha}_{\mathrm{mm}}^{\mathrm{co}}. \tag{4.7}$$

For the non-transparent side of an omega transparent metasurface, reflected and transmitted waves read

$$\mathbf{E}_{\mathrm{r}} = \frac{2\omega}{S}\widehat{\Omega}\,\mathbf{E}_{\mathrm{inc}}, \qquad \mathbf{E}_{\mathrm{t}} = \mathbf{E}_{\mathrm{inc}}. \tag{4.8}$$

Assuming passivity, it is clear that the omega coupling coefficient must also be zero. However, relaxing the passivity restriction by letting the metasurface be active opens new possibilities. It is feasible to design a reciprocal active one-way transparent metasurface which enables control over the co-polarized reflection (controlled by the value of the omega coupling) for the wave hitting the non-transparent side of the metasurface. The requirement of reciprocity is very limiting, because it imposes full transmissions from both sides.

Now let us consider nonreciprocal cases. It can be easily seen from (4.6) that any passive one-way transparent sheet must have zero reflections from both sides. This is because the total power of two waves (the reflected wave from the non-transparent side and the wave transmitted from the transparent side) is not equal to the sum of the powers of these two waves due to their interference. Thus, a passive one-way transparent sheet allows control only over the transmission coefficients for waves coming from the opposite direction (the polarization state and phase delays of transmitted waves can be engineered with complete freedom). Let us consider a transparent layer possessing "moving" coupling. The one-way transparency conditions in (4.5) take the form

$$\eta_0\widehat{\alpha}_{\mathrm{ee}}^{\mathrm{co}} = \widehat{V} = \frac{1}{\eta_0}\widehat{\alpha}_{\mathrm{mm}}^{\mathrm{co}}, \quad \eta_0\widehat{\alpha}_{\mathrm{ee}}^{\mathrm{cr}} = \frac{1}{\eta_0}\widehat{\alpha}_{\mathrm{mm}}^{\mathrm{cr}} = 0. \tag{4.9}$$

The reflected and transmitted waves due to an incident plane wave illuminating the non-transparent side of the metasurface read

$$\mathbf{E}_{\mathrm{r}} = 0, \qquad \mathbf{E}_{\mathrm{t}} = \left(1 - \frac{j2\omega}{S}\widehat{V}\right)\mathbf{E}_{\mathrm{inc}}. \tag{4.10}$$

It is clear that a moving one-way transparent metasurface can be designed so as to enable controllable amplitude and phase of the transmitted fields for waves hitting the non-transparent side of the metasurface. A special example of this scenario is a single-layer isolator (for a lossy metasurface) which was discussed in Sec. 2.2.

It can be seen from (4.6) that a passive Tellegen transparent metasurface is not possible and controlling cross-polarized reflections from the non-transparent side is only possible in an active Tellegen transparent metasurface. Generally, to control reflections from the non-transparent

side in an asymmetric transparent metasurface, the structure must be active. Conceptually, it is possible to fully absorb the power incident from the non-transparent side and produce secondary ("reflected") waves using active elements.

4.1.3 Contributions of this thesis (summary of related publications)

Publication [IV] introduces the general theory of bianisotropic transparent metasurfaces which are fully transparent from one of their sides while providing controllable functionalities for waves illuminating their non-transparent sides. We explore, under the limitations imposed by reciprocity and passivity, all possible functionalities for asymmetric transparent metasurfaces with different classes of electromagnetic couplings.

4.2 All-angle Huygens' metasurfaces

4.2.1 Theory

As it was mentioned before, most of the recently presented metasurfaces are angular– and polarization-sensitive which dramatically limits their functionalities. This means that as soon as the polarization of incident wave changes or the incidence angle deviates from the designed value reflections from the metasurfaces appear. Let us think of a more efficient metasurface which remains a Huygens' metasurface independent of the incidence angle and polarization of the excitation.

Consider a metasurface possessing no bianisotropic coupling located in free space. Impedance boundary conditions can be utilized to model such a metasurface [2]

$$\mathbf{E}_{\mathrm{av}} = \eta_0 \overline{\overline{Z}}_{\mathrm{e}} \cdot \mathbf{J}_{\mathrm{e}}, \quad \eta_0 \overline{\overline{Z}}_{\mathrm{m}} \cdot \mathbf{H}_{\mathrm{av}} = \mathbf{J}_{\mathrm{m}}. \tag{4.11}$$

Here $\mathbf{E}_{\mathrm{av}}$ and $\mathbf{H}_{\mathrm{av}}$ are the surface-averaged tangential electric and magnetic fields in the metasurface plane, $\mathbf{J}_{\mathrm{e}}$ and $\mathbf{J}_{\mathrm{m}}$ are the electric and magnetic surface current densities, and $\overline{\overline{Z}}_{\mathrm{e}}$ and $\overline{\overline{Z}}_{\mathrm{m}}$ are the dyadic electric and magnetic surface impedances normalized to the free-space impedance η_0. For a uniaxial metasurface with no bianisotropic coupling, where the only preferred direction is given by the unit vector normal to the surface $\mathbf{n}$, the

surface impedances can be written in the form [2],

$$\overline{\overline{Z}}_{\mathrm{e,m}} = Z_{\mathrm{e,m}}^{\mathrm{TM}} \frac{\mathbf{k}_{\mathrm{t}}\mathbf{k}_{\mathrm{t}}}{k_{\mathrm{t}}^2} + Z_{\mathrm{e,m}}^{\mathrm{TE}} \frac{\mathbf{n}\times\mathbf{k}_{\mathrm{t}}\mathbf{n}\times\mathbf{k}_{\mathrm{t}}}{k_{\mathrm{t}}^2}, \tag{4.12}$$

where $\mathbf{k}_{\mathrm{t}}$ is the tangential component of the wave vector of the incident plane wave[1]. Here the indices TM and TE correspond to the two orthogonal polarizations of the incident fields. The length of the tangential component of the wave vector relates to the angle of incidence θ as $k_{\mathrm{t}} = k_0 \sin\theta$ (k_0 is the free-space wavenumber). To obtain the reflection and transmission coefficients from this metasurface, we can simply satisfy the boundary conditions given in (4.11), which results in

$$\begin{aligned}
\overline{\overline{R}} = &\frac{Z_{\mathrm{e}}^{\mathrm{TM}} Z_{\mathrm{m}}^{\mathrm{TM}} - \cos^2\theta}{\left(Z_{\mathrm{e}}^{\mathrm{TM}} + \dfrac{\cos\theta}{2}\right)\left(Z_{\mathrm{m}}^{\mathrm{TM}} + 2\cos\theta\right)} \frac{\mathbf{k}_{\mathrm{t}}\mathbf{k}_{\mathrm{t}}}{k_{\mathrm{t}}^2} \\
&+ \frac{Z_{\mathrm{e}}^{\mathrm{TE}} Z_{\mathrm{m}}^{\mathrm{TE}} - \dfrac{1}{\cos^2\theta}}{\left(Z_{\mathrm{e}}^{\mathrm{TE}} + \dfrac{1}{2\cos\theta}\right)\left(Z_{\mathrm{m}}^{\mathrm{TE}} + \dfrac{2}{\cos\theta}\right)} \frac{\mathbf{n}\times\mathbf{k}_{\mathrm{t}}\mathbf{n}\times\mathbf{k}_{\mathrm{t}}}{k_{\mathrm{t}}^2}, \\
\overline{\overline{T}} = &\frac{\cos\theta\left(2Z_{\mathrm{e}}^{\mathrm{TM}} - \dfrac{Z_{\mathrm{m}}^{\mathrm{TM}}}{2}\right)}{\left(Z_{\mathrm{e}}^{\mathrm{TM}} + \dfrac{\cos\theta}{2}\right)\left(Z_{\mathrm{m}}^{\mathrm{TM}} + 2\cos\theta\right)} \frac{\mathbf{k}_{\mathrm{t}}\mathbf{k}_{\mathrm{t}}}{k_{\mathrm{t}}^2} \\
&+ \frac{\dfrac{1}{\cos\theta}\left(2Z_{\mathrm{e}}^{\mathrm{TE}} - \dfrac{Z_{\mathrm{m}}^{\mathrm{TE}}}{2}\right)}{\left(Z_{\mathrm{e}}^{\mathrm{TE}} + \dfrac{1}{2\cos\theta}\right)\left(Z_{\mathrm{m}}^{\mathrm{TE}} + \dfrac{2}{\cos\theta}\right)} \frac{\mathbf{n}\times\mathbf{k}_{\mathrm{t}}\mathbf{n}\times\mathbf{k}_{\mathrm{t}}}{k_{\mathrm{t}}^2}.
\end{aligned} \tag{4.13}$$

It can be easily seen from these equations that the required conditions for an all-angle Huygens' metasurface (i.e., $R_{\mathrm{TM}}(\theta) = R_{\mathrm{TE}}(\theta) = 0$ for all θ) read

$$Z_{\mathrm{e}}^{\mathrm{TM}} Z_{\mathrm{m}}^{\mathrm{TM}} = \cos^2\theta, \quad Z_{\mathrm{e}}^{\mathrm{TE}} Z_{\mathrm{m}}^{\mathrm{TE}} = \frac{1}{\cos^2\theta}. \tag{4.14}$$

Satisfying these conditions, the transmission coefficient in (4.13) can be rewritten as

$$\overline{\overline{T}} = \frac{Z_{\mathrm{e}}^{\mathrm{TM}} - \dfrac{\cos\theta}{2}}{Z_{\mathrm{e}}^{\mathrm{TM}} + \dfrac{\cos\theta}{2}} \frac{\mathbf{k}_{\mathrm{t}}\mathbf{k}_{\mathrm{t}}}{k_{\mathrm{t}}^2} + \frac{Z_{\mathrm{e}}^{\mathrm{TE}} - \dfrac{1}{2\cos\theta}}{Z_{\mathrm{e}}^{\mathrm{TE}} + \dfrac{1}{2\cos\theta}} \frac{\mathbf{n}\times\mathbf{k}_{\mathrm{t}}\mathbf{n}\times\mathbf{k}_{\mathrm{t}}}{k_{\mathrm{t}}^2}. \tag{4.15}$$

It can be seen from this equation that for a lossless metasurface (purely imaginary $Z_{\mathrm{e,m}}^{\mathrm{TM,TE}}$) the amplitude of the transmission coefficient is unity, and its phase can be fully controlled (in the range $0 - 2\pi$) varying the electric and magnetic impedances of the layer. Here are two important points to be noted. First, an all-angle Huygens' metasurface should be

[1] $\mathbf{vw}$ forms a dyadic product of two vectors $\mathbf{v}$ and $\mathbf{w}$.

spatially dispersive. Second, possible realizations for such a metasurface are not unique. The latter statement holds because although the product of the surface electric and magnetic impedances should have the $\cos^2\theta$ (for the TM case) or $1/\cos^2\theta$ (for the TE case) dependency, each of them individually can have any arbitrary angular dependency. Getting inspired by earlier work on uniaxial perfectly matched layers [89], as a possible realization we propose an electrically thin uniaxial material layer in free space. The layer has the thickness d and is characterized by the material parameters $\overline{\overline{\epsilon}} = \epsilon_0(\epsilon_\mathrm{t}\overline{\overline{I}}_\mathrm{t}+\epsilon_\mathrm{n}\mathbf{nn})$, $\overline{\overline{\mu}} = \mu_0(\mu_\mathrm{t}\overline{\overline{I}}_\mathrm{t}+\mu_\mathrm{n}\mathbf{nn})$, where $\overline{\overline{I}}_\mathrm{t}$ is the 2D unit dyadic defined in the layer plane. The surface impedances for such a layer can be derived following the steps described in [2]. Assuming $\epsilon_\mathrm{n}\mu_\mathrm{t} = 1$ and $\epsilon_\mathrm{t}\mu_\mathrm{n} = 1$, and $k_0 d \ll 2/|\sqrt{\epsilon_\mathrm{t}\mu_\mathrm{t}}|$, the sheet impedances for such a layer can be approximated as

$$\begin{aligned}\overline{\overline{Z}}_\mathrm{e} &= -\frac{j}{k_0 d\epsilon_\mathrm{t}\cos\theta}\left[\cos\theta\frac{\mathbf{k}_\mathrm{t}\mathbf{k}_\mathrm{t}}{k_\mathrm{t}^2}+\frac{1}{\cos\theta}\frac{\mathbf{n}\times\mathbf{k}_\mathrm{t}\mathbf{n}\times\mathbf{k}_\mathrm{t}}{k_\mathrm{t}^2}\right],\\ \overline{\overline{Z}}_\mathrm{m} &= jk_0 d\mu_\mathrm{t}\cos\theta\left[\cos\theta\frac{\mathbf{k}_\mathrm{t}\mathbf{k}_\mathrm{t}}{k_\mathrm{t}^2}+\frac{1}{\cos\theta}\frac{\mathbf{n}\times\mathbf{k}_\mathrm{t}\mathbf{n}\times\mathbf{k}_\mathrm{t}}{k_\mathrm{t}^2}\right].\end{aligned} \tag{4.16}$$

These surface impedances satisfy the requirements for all-angle Huygens' metasurfaces in (4.14). For such a layer, conditions for required material parameters read [see (4.14) and (4.16)]

$$\epsilon_\mathrm{t} = \mu_\mathrm{t}, \quad \epsilon_\mathrm{n}\mu_\mathrm{t} = 1, \quad \epsilon_\mathrm{t}\mu_\mathrm{n} = 1, \quad k_0 d \ll 2/|\sqrt{\epsilon_\mathrm{t}\mu_\mathrm{t}}|. \tag{4.17}$$

Although the impedances in (4.16) satisfy the required conditions for an all-angle Huygens' metasurface [see (4.14)], due to the last condition in (4.17), thin uniaxial layer will not be able to provide arbitrary transmission phase [see (4.15)]. However, stacking a number of these all-angle Huygens' metasurfaces, we can get any arbitrary transmission phase.

4.2.2 Contributions of this thesis (summary of related publications)

Publication [V] presents the general theory of angularly-independent Huygens' metasurfaces. We study the required conditions for an all-angle Huygens' metasurface capable of tailoring the transmitted waves at will. We investigate uniaxial electrically thin layers as a possible option for the angularly-independent Huygens' metasurfaces. We conclude that although a thin uniaxial layer can be designed so as to serve as an angularly-independent Huygens' metasurface, it will not be able to arbitrarily tailor the transmitted wave and a stack of these all-angle Huygens' metasurfaces is needed to provide any arbitrary transmission phase.

5. $\mathcal{PT}$-symmetric metasurfaces

The phenomenon of tunneling electromagnetic waves through opaque layers has recently attracted considerable attention. Tunneling structures based on an extremely high negative permittivity layer coated by high positive permittivity layers [90], a negative permittivity slab sandwiched between birefringence layers [86], conjugate matched pair of epsilon-negative and mu-negative slabs [85], and also an epsilon-negative slab paired with a double-positive uniaxial slab [91] have been reported. Recently, it was revealed that the phenomenon of electromagnetic wave tunneling can happen through electrically long distances [92]. It was shown that putting an extremely high negative permittivity layer and an extremely high negative permeability layer far apart, electromagnetic waves can still tunnel through. But what if the incident electromagnetic wave is "teleported" from the input of the structure to its output instead of getting tunneled? Can we design a structure which absorbs electromagnetic waves at one surface and recreates it at another place far away from the first surface?

It seems that this phenomenon may be realizable employing a new class of artificial structures based on parity-time-symmetric ($\mathcal{PT}$-symmetric) systems, which has recently attracted considerable research attention. In these structures, controllable combination of lossy and active components, while the overall response can remain lossless, provides unprecedented control of electromagnetic wavefronts [93–96]. Recently, a unidirectional cloaking structure based on $\mathcal{PT}$-symmetric systems was introduced [96]. In that design, half of the structure, which is lossy, fully absorbs the incident wave and the active half of the structure repeats it behind the cloak. It was shown that in this structure a small amount of coupling is enough to deliver the required information about the incident wave from the lossy half to the active half of the structure. Inspired by this work, we propose and investigate an idea of $\mathcal{PT}$-symmetric teleportation through a highly

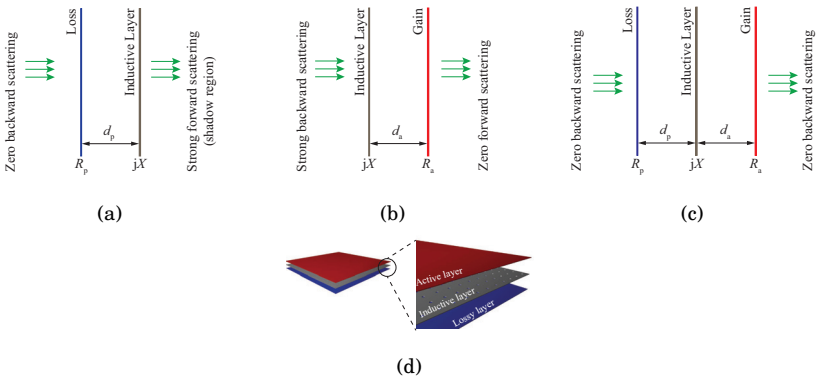

Figure 5.1. Topology of a generic structure with (a) zero reflected power, (b) absence of shadow, and (c) zero total scattering. (d) 3D schematic for a $\mathcal{PT}$-symmetric tunnelling structure.

reflective metal sheet perforated with a subwavelength array of tiny holes.

5.1 Design principles

Consider a lossless metallic layer perforated with a 2D periodic array of electrically small holes with a period much smaller than the free-space wavelength (λ_0). Such a layer would have a very small surface inductance (in our design, we assume the surface reactance is $X = 0.01\Omega$). If an incident plane wave normally illuminates this sheet, 99.98% of the incident power will be reflected and only a negligible amount of the incident power, i.e., 0.02% will be transmitted through the sheet. This means that such a layer strongly reflects the incident wave and creates a deep shadow behind it.

The main question which we are going to address is: How can one manipulate the scattering properties of this structure by introducing controllable amounts of loss and gain into the system. Let us first think about how we can eliminate the reflections from this structure. The only way to eliminate the backward scattering from this highly reflective metallic sheet is to absorb the incident wave. Since the inductive layer works as an almost ideal lossless metallic layer, to absorb the incident wave, one can easily put a resistive sheet $R_\mathrm{p} = \eta_0$ at the distance of $d_\mathrm{p} = 7.5\,\mathrm{mm} = \lambda_0/4$ in front of the metallic layer [see Fig. 5.1(a)], resembling the Salisbury absorber [97]. This way, we can eliminate the backward scattering from the metallic sheet.

As it was mentioned before, the metallic sheet creates a complete shadow

behind it. Since the metallic sheet reflects almost all the impinging power, in order to engineer the shadow, we need a secondary source behind the metallic film. As the secondary source, let us put an active layer with $R_{\rm a} = -\eta_0$ at the distance of $d_{\rm a} = 7.5\,{\rm mm} = \lambda_0/4$ from the inductive layer behind it [see Fig. 5.1(b)]. Here, the active side should somehow get information about the frequency, phase, and amplitude of the impinging wave in order to be able to produce a plane wave behind the structure with desirable characteristics. In this structure small field penetration through the array of holes will reach the active layer establishing a resonating feedback loop between the inductive and active sheets. This electromagnetic whispering between the inductive and active layers will continue until this *anti-absorbing structure* reproduces the desirable propagating wave behind it. With the design parameters mentioned above, this structure fully reflects the incident wave while reproducing a transmitted wave with the transmission coefficient of $T = -j2$.

Up to now, we studied two different scenarios: A passive resonator capable of eliminating the backward scattering and an active resonator which enables engineering the shadow behind the structure. To eliminate both the backward scattering and the shadow, we can combine these two resonators in a single structure, forming a $\mathcal{PT}$-symmetric structure [see Figs. 5.1(c) and 5.1(d)]. Figures 5.2(a) and 5.2(b) show that, at the operating frequency of the structure $f_0 = 10$ GHz, this structure is capable of recreating the incident wave (with the same frequency and amplitude) behind it without producing any backward scattering. It should be noted that the incident and transmitted waves are out of phase which means that the structure works as a cloak. Indeed, there is no reflected wave and no forward-scattered wave. In order to cloak the metallic layer for a given TM polarized incident wave with angle of incidence $\theta_{\rm i}$, design parameters should be adjusted accordingly, i.e., $R_{\rm p} = -R_{\rm a} = \eta_0 \cos\theta_{\rm i}$ and $d_{\rm p} = d_{\rm a} = \lambda_0/(4\cos\theta_{\rm i})$ [see Figs. 5.2(c), 5.2(d), and 5.2(e)]. Figures 5.2(a), 5.2(b), 5.2(f), 5.2(g), and 5.2(h) show that replication of the incident wave behind the structure happens in an angularly and spectrally selective fashion.

It is quite interesting to investigate what reason causes this phenomenon and what is the physics behind it. Figure 5.3(a) shows the transmission-line schematic for this $\mathcal{PT}$-symmetric structure. It is seen that at the resonance frequency the inductive impedance is shorted out. This phenomenon implies a very important point: At the resonance frequency, the

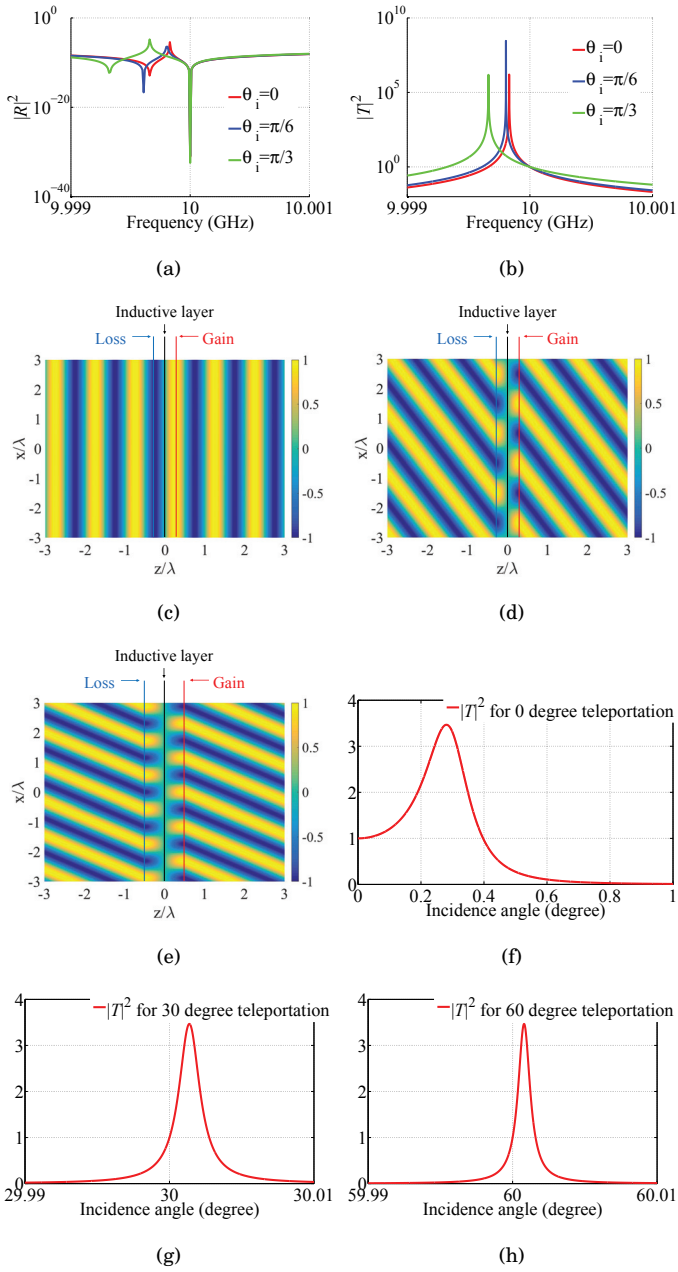

Figure 5.2. $\mathcal{PT}$-symmetric structure [see Fig. 5.1(c)]: (a) and (b) Frequency responses for the case of $\theta_{\rm i} = 0$, $\theta_{\rm i} = \pi/6$, and $\theta_{\rm i} = \pi/3$. (c) Electric field distribution for the case of $\theta_{\rm i} = 0$. (d) Electric field distribution for the case of $\theta_{\rm i} = \pi/6$. (e) Electric field distribution for the case of $\theta_{\rm i} = \pi/3$. Angular response for (f) 0-degree, (g) 30-degree, and (h) 60-degree teleportation structures (Here, we assume that the sheet resistances are angular independent).

passive and active sides are completely isolated and there is no connection between these two parts of the structure. The main question which

comes to mind is how the active part of the structure can replicate the incident wave behind the structure while these two parts are electromagnetically disconnected. Do we have tunnelling mechanism or teleportation mechanism? In other words, do we tunnel the incident wave through the structure or we fully absorb it at the input and recreate it with the same characteristics at the output of the structure? To answer this question we can look at the time domain simulation of the structure.

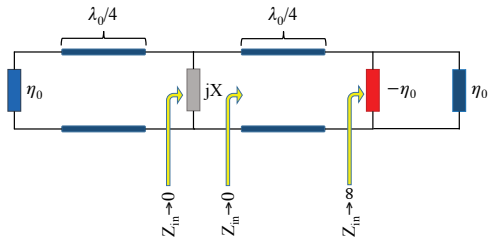

(a)

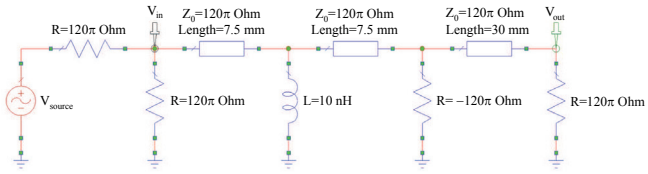

(b)

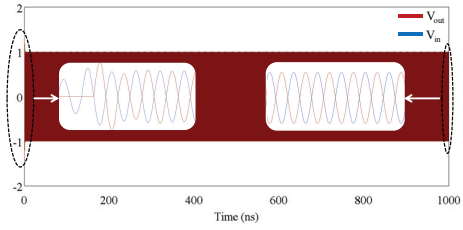

(c)

Figure 5.3. $\mathcal{PT}$-symmetric structure [see Fig. 5.1(c)]: (a) Transmission-line schematic, (b) circuit model, and (c) time-domain simulation.

Figures 5.3(b) and 5.3(c) show the circuit model of the structure and the results of its time-domain simulation, respectively. It is seen that we basically have both tunnelling and teleportation regimes in the structure. When we start illuminating the structure, during the transient time period (before getting to the steady state) there is a weak tunnelling (plane wave propagation) between the passive and active sides which is responsible for delivering the information of the incident wave to the active side. However, as soon as the structure approaches the steady state, there is no

tunnelling between these two parts [see the transmission-line schematic in Fig. 5.3(a)] and the structure is in the teleportation regime.

As it can be seen from Fig. 5.2(b), a huge amplification in transmission may happen at frequencies close to the operating frequency of the structure (i.e., $f_0 = 10$ GHz). This amplification phenomenon, which is of tunneling nature, depends on the reactance of the inductive layer and may be tuned to any frequency close to or far from the one in which teleportation phenomenon happens. Similar phenomenon happens when we deviate the angle of incidence from the designed value [see Figs. 5.2(f), 5.2(g), and 5.2(h)].

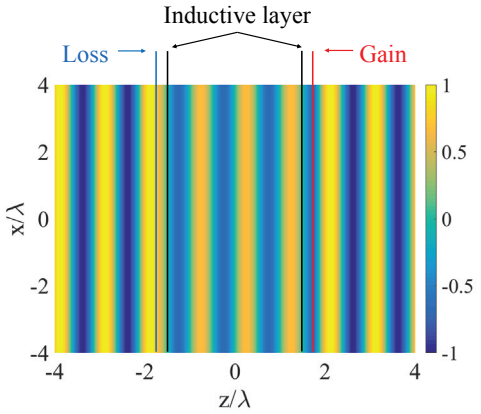

Figure 5.4. Field distribution for the case of teleporting incident wave through a distance.

At this point, there comes an interesting question whether it is possible to locate lossy and active parts of the structure far away from each other and still teleport the incident wave? Figure 5.4 shows a $\mathcal{PT}$-symmetric structure in which the lossy and active parts are located at the distance $3\lambda_0$. Electric field distribution shows that incident electromagnetic waves can fully teleport through the structure. It can be seen that at the steady state regime there is no power flow from the passive side toward the active one, instead, there is a standing wave between two inductive layers. It should be noted that the same phenomena can happen for longer distances $d_t \approx n\lambda_0/2$ where n is an integer.

Here we discussed the pair of Salisbury-type absorber and anti-absorber. However, the same concept can be applied to a pair of a Dallenbach absorber and an anti-absorber [98]. This way we can realize electrically thin angular and frequency filters.

5.2 Contributions of this thesis (summary of related publications)

Publication [VI] discusses the scattering properties of a new $\mathcal{PT}$-symmetric structure. We show that putting an active layer behind a highly reflective metallic sheet perforated with a 2D subwavelength array of tiny holes, one can engineer the shadow behind the reflective sheet. It is shown that a little amount of field penetration through the highly reflective metallic sheet is enough to establish a feedback loop between the inductive and active layers which is responsible to delivering the information of the incident wave to the active layer. We also show that plane waves can be fully "teleported" through the thin metallic layer, assisted by a pair of lossy and active sheets in front and behind the screen.

6. Conclusions

This thesis contributes to the development of functional metasurfaces. We have studied OBT absorbing metasurfaces, OBT reflecting metasurfaces, Huygens' metasurfaces, and $\mathcal{PT}$-symmetric metasurfaces.

We first introduced the general theory of OBT absorbing metasurfaces composed of single arrays of polarizable inclusions. We studied the concept of both symmetric and asymmetric absorbing metasurfaces. The design possibilities offered by the particles of all four fundamental classes of bianisotropic inclusions: reciprocal chiral and omega particles and nonreciprocal Tellegen and moving particles were explored.

We next introduced the general concept of OBT reflecting metasurfaces. We investigated the physical requirements to realize symmetric and asymmetric OBT mirrors. It was shown that metasurfaces with bianisotropic omega coupling are required to get asymmetric response in reflection phase for plane waves hitting their different sides.

The third part of the thesis was devoted to the general theory of Huygens' metasurfaces. We first presented the concept of symmetric and asymmetric transparent metasurfaces. All possible functionalities considering limitations due to reciprocity and passivity were investigated. Furthermore, we studied the concept of all-angle Huygens' metasurfaces. These metasurfaces do not produce any reflections for arbitrary illuminations, while they are fully able to tailor transmitted waves.

In the last part of the thesis, we studied the concept of one-dimensional cloak based on $\mathcal{PT}$-symmetric systems. We showed that electromagnetic plane waves can be fully recreated behind a thin, nearly fully reflective sheet, assisted by a pair of $\mathcal{PT}$-symmetric lossy and active sheets in front and behind the screen. It was shown that the same concept can be applied in order to cloak a structure composed of two parallel highly-reflective metallic sheets located far away from each other. This phenomenon looks

like teleporting electromagnetic waves (absorbing electromagnetic waves at one point and recreating them at a different point) through electrically long distances, however it should be noted that the restored fields have the same phase as the incident wave at the place of the active sheet (similar to cloaking phenomenon).

Throughout the thesis we have theoretically introduced different functional metasurfaces. We believe that the results reported in this thesis can contribute to a big step forward in the field of metasurfaces and open up new and more revealing directions for research. Studying angular dependency of OBT absorbing, OBT reflecting, and transparent metasurfaces, realizing these metasurfaces in different frequency ranges, and designing Dallenbach-type $\mathcal{PT}$-symmetric metasurfaces could be some interesting topics for future research works.

References

[1] S. Kinoshita and S. Yoshioka, "Structural colors in nature: The role of regularity and irregularity in the structure", *ChemPhysChem*, vol. 6, pp. 1442–1459, 2005.

[2] S. A. Tretyakov, *Analytical modeling in applied electromagnetics,* Norwood, MA: Artech House, 2003.

[3] G. V. Eleftheriades and K. G. Balmain, Eds., *Negative-refraction metamaterials: fundamental principles and applications,* Hoboken, NJ: John Wiley & Sons, 2005.

[4] C. Caloz and T. Itoh, *Electromagnetic metamaterials: Transmission line theory and microwave applications,* Hoboken, NJ: John Wiley & Sons, 2006.

[5] A. Sihvola, "Metamaterials in electromagnetics", *Metamaterials*, vol. 1, no. 1, pp. 2–11, 2007.

[6] N. Engheta and R. W. Ziolkowski, Eds., *Electromagnetic metamaterials: Physics and engineering explorations,* Wiley-IEEE Press, 2006.

[7] V. M. Shalaev and A. K. Sarychev, *Electrodynamics of metamaterials,* World Scientific Publishing Company, 2007.

[8] R. Marques, F. Martin, and M. Sorolla, *Metamaterials with negative parameters: Theory, design and microwave applications,* Wiley Series in Microwave and Optical Engineering, Wiley-Interscience, 2008.

[9] P. Markos and C. M. Soukoulis, *Wave propagation: From electrons to photonic crystals and left-handed materials,* Princeton University Press, 2008.

[10] F. Capolino, Ed., *Handbook of artificial materials,* New York: CRC Press, 2009.

[11] B. Banerjee, *An introduction to metamaterials and waves in composites,* Boca Raton: CRC Press, 2011.

[12] J. B. Pendry, D. Schurig, and D. R. Smith, "Controlling electromagnetic fields", *Science*, vol. 312, pp. 1780–1782, 2006.

[13] U. Leonhardt, "Optical conformal mapping", *Science*, vol. 312, pp. 1777–1780, 2006.

[14] V. M. Shalaev, "Optical negative-index metamaterials", *Nat. Photonics*, vol. 1, pp. 41–48, 2007.

[15] C. M. Soukoulis and M. Wegener, "Past achievements and future challenges in the development of three-dimensional photonic metamaterials", *Nat. Photonics*, vol. 5, pp. 523–530, 2011.

[16] A. E. Caswell, *An outline of physics,* New York: The Macmillan Company, 1929.

[17] C. Huygens, *Traite de la lumiere,* 1690. Translated into English by S. P. Thompson, London, 1912 and reprinted by the University of Chicago Press.

[18] A. E. H. Love, "The integration of the equations of propagation of electric waves", *Phil. Trans. Roy. Soc. London, Ser. A*, vol. 197, pp. 1–45, 1901.

[19] S. A. Schelkunoff, "Some equivalence theorems of electromagnetics and their application to radiation problems", *Bell System Tech. J.*, vol. 15, pp. 92–112, 1936.

[20] E. F. Kuester, M. A. Mohamed, M. Piket-May and C. L. Holloway, "Averaged transition conditions for electromagnetic fields at a metafilm", *IEEE Trans. Antennas Propag.*, vol. 51, no. 10, pp. 2641–2651, 2003.

[21] C. L. Holloway, M. A. Mohamed, E. F. Kuester, and A. Dienstfrey, "Reflection and transmission properties of a metafilm: With an application to a controllable surface composed of resonant particles", *IEEE Trans. Electromag. Compat.*, vol. 47, no. 4, pp. 853–865, 2005.

[22] A. V. Kildishev, A. Boltasseva, and V. M. Shalaev, "Planar photonics with metasurfaces", *Science*, vol. 339, no. 6125, p. 1232009, 2013.

[23] Y. Zhao, X. -X. Liu, and A. Alù, "Recent advances on optical metasurfaces", *J. Opt.*, vol. 16, p. 123001, 2014.

[24] M. Selvanayagam and G. V. Eleftheriades, "Discontinuous electromagnetic fields using orthogonal electric and magnetic currents for wavefront manipulation", *Opt. Expr.*, vol. 21, no. 12, pp. 14409–14429, 2013.

[25] C. Holloway, E. F. Kuester, J. Gordon, J. O'Hara, J. Booth, and D. Smith, "An overview of the theory and applications of metasurfaces: The two-dimensional equivalents of metamaterials", *IEEE Antennas Propag. Mag.*, vol. 54, no. 2, pp. 10–35, 2012.

[26] N. Yu and F. Capasso, "Flat optics with designer metasurfaces", *Nature Mater.*, vol. 13, pp. 139–150, 2014.

[27] D. L. Sounas, T. Kodera, and C. Caloz, "Electromagnetic modeling of a magnet-less non-reciprocal gyrotropic metasurface", *IEEE Trans. Antennas Propag.*, vol. 61, no. 1, pp. 221–231, 2013.

[28] C. Pfeiffer, C. Zhang, V. Ray, L. J. Guo, and A. Grbic, "High performance bianisotropic metasurfaces: Asymmetric transmission of light", *Phys. Rev. Lett.*, vol. 113, no. 2, p. 023902, 2014.

[29] H. Lamb, "On the reflection and transmission of electric waves by a metallic grating", *Proc. Lond. Math. Soc.*, vol. 29, pp. 523–544, 1898.

[30] G. G. MacFarlane, "Surface impedance of an infinite parallel-wire grid at oblique angles of incidence", *J. Inst. EIec. Eng.*, vol. 93, pp. 1523–1527, 1946.

[31] J. R. Wait, "Reflection at arbitrary incidence from a parallel wire grid", *Appl. Sci. Res., B*, vol. 4, pp. 393–400, 1954.

[32] M. I. Kontorovich, V. Yu. Petrunkin, N. A. Esepkina, and M. I. Astrakhan, "Reflection factor of a plane electromagnetic wave reflecting from a plane wire grid", *Radio Eng. Electron Phys.*, vol. 7, pp. 222–231, 1962.

[33] B. A. Munk, *Frequency selective surfaces: Theory and design*, New York: Wiley, 2000.

[34] G. Marconi and C. S. Franklin, "Reflector for use in wireless telegraphy and telephony", U.S. Patent 1 301 473 (22 April 1919).

[35] D. M. Pozar, S. D. Targonski, and H. D. Syrigos, “Design of millimeter wave microstrip reflectarrays”, *IEEE Trans. Antennas Propag.*, vol. 45, no. 2, pp. 287–296, 1997.

[36] C. G. M. Ryan, M. R. Chaharmir, J. Shaker, J. R. Bray, Y. M. M. Antar, and A. Ittipiboon, “A wideband transmitarray using dual-resonant double square rings,” *IEEE Trans. Antennas Propag.,* vol. 58, no. 5, pp. 1486–1493, 2010.

[37] Y. Ra’di, V. S. Asadchy and S. A. Tretyakov, “Tailoring reflections from thin composite metamirrors”, *IEEE Trans. Antennas Propag.*, vol. 62, no. 7, pp. 3749–3760, 2014.

[38] V. S. Asadchy, Y. Ra’di, J. Vehmas, and S. A. Tretyakov, “Functional metamirrors using bianisotropic elements”, *Phys. Rev. Lett.*, vol. 114, n. 9, p. 095503, 2015.

[39] B. H. Fong, J. S. Colburn, J. J. Ottusch, J. L. Visher, and D. F. Sievenpiper, “Scalar and tensor holographic artificial impedance surfaces,” *IEEE Trans. Antennas Propag.,* vol. 58, no. 10, pp. 3212–3221, 2010.

[40] G. Minatti, S. Maci, P. De Vita, A. Freni, and M. Sabbadini, “A circularly-polarized isoflux antenna based on anisotropic metasurface,” *IEEE Trans. Antennas Propag.,* vol. 60, no. 11, pp. 4998–5009, 2012.

[41] S. Pandi, C. A. Balanis, and C. R. Birtcher, “Design of scalar impedance holographic metasurfaces for antenna beam formation with desired polarization,” *IEEE Trans. Antennas Propag.,* vol. 63, no. 7, pp. 3016–3024, 2015.

[42] C. Pfeiffer and A. Grbic, “Metamaterial Huygens’ surfaces: Tailoring wave fronts with reflectionless sheets”, *Phys. Rev. Lett.*, vol. 110, p. 197401, 2013.

[43] C. Pfeiffer, N. K. Emani, A. M. Shaltout, A. Boltasseva, V. M. Shalaev, and A. Grbic, “Efficient light bending with isotropic metamaterial Huygens’ surfaces”, *Nano Lett.*, vol. 14, pp. 2491–2497, 2014.

[44] Y. Ra’di, V. S. Asadchy, and S. A. Tretyakov, “One-way transparent sheets”, *Phys. Rev. B*, vol. 89, n. 7, p. 075109, 2014.

[45] Y. Ra'di, V. S. Asadchy, and S. A. Tretyakov, "Total absorption of electromagnetic waves in ultimately thin layers", *IEEE Trans. Antennas Propag.*, vol. 61, no. 9, pp. 4606–4614, 2013.

[46] F. Monticone, N. M. Estakhri, and A. Alù, "Optical transmission with a composite metascreen", *Phys. Rev. Lett.*, vol. 110, no. 20, p. 203903, 2013.

[47] M. Decker, I. Staude, M. Falkner, J. Dominguez, D. N. Neshev, I. Brener, T. Pertsch, and Y. S. Kivshar, "High-efficiency dielectric Huygens' surfaces", *Adv. Optical Mater.*, vol. 3, no. 6, pp. 813–820, 2015.

[48] S. Sun, K. -Y. Yang, C. -M. Wang, T. -K. Juan, W. T. Chen, C. Y. Liao, Q. He, S. Xiao, W. -T. Kung, G. -Y. Guo, L. Zhou, and D. P. Tsai, "High-efficiency broadband anomalous reflection by gradient metasurfaces", *Nano Lett.*, vol. 12, n. 12, pp. 6223–6229, 2012.

[49] A. Pors, M. G. Nielsen, R. L. Eriksen, and S. I. Bozhevolnyi, "Broadband focusing flat mirrors based on plasmonic gradient metasurfaces", *Nano Lett.*, vol. 13, n. 2, pp. 829–834, 2013.

[50] M. Esfandyarpour, E. C. Garnett, Y. Cui, M. D. McGehee, and M. L. Brongersma, "Metamaterial mirrors in optoelectronic devices", *Nat. Nanotechnol.*, vol. 9, pp. 542–547, 2014.

[51] M. Veysi, C. Guclu, O. Boyraz, and F. Capolino, "Thin anisotropic metasurfaces for simultaneous light focusing and polarization manipulation", *JOSA B*, vol. 32, no. 2, pp. 318–323, 2015.

[52] C. Saeidi and D. Weide, "Wideband plasmonic focusing metasurfaces", *Appl. Phys. Lett.*, vol. 105, p. 053107, 2014.

[53] C. L. Holloway, A. Dienstfrey, E. F. Kuester, J. F. O'Hara, A. K. Azad and A. J. Taylor, "A discussion on the interpretation and characterization of metafilms/metasurfaces: The two-dimensional equivalent of metamaterials", *Metamaterials*, vol. 3, no. 2, pp. 100–112, 2009.

[54] C. R. Simovski, "On electromagnetic characterization and homogenization of nanostructured metamaterials", *J. Opt.*, vol. 13, no. 1, p. 013001, 2011.

[55] D. Morits and C. Simovski, “Electromagnetic characterization of planar and bulk metamaterials: A theoretical study”, *Phys. Rev. B*, vol. 82, p. 165114, 2010.

[56] D. R. Smith, S. Schultz, P. Markoš, and C. M. Soukoulis, “Determination of effective permittivity and permeability of metamaterials from reflection and transmission coefficients”, *Phys. Rev. B*, vol. 65, no. 19, p. 195104, 2002.

[57] T. Niemi, A. Karilainen, and S. Tretyakov, “Synthesis of polarization transformers”, *IEEE Trans. Antennas Propag.*, vol. 61, no. 6, pp. 3102–3111, June 2013.

[58] M. Y. Koledintseva, J. Huang, J. L. Drewniak, R. E. DuBroff, and B. Archambeault, “Modeling of metasheets embedded in dielectric layers”, *Prog. Electromagn. Res. B*, vol. 44, pp. 89–116, 2012.

[59] M. Albooyeh, D. Morits, and C. R. Simovski, “Electromagnetic characterization of substrated metasurfaces”, *Metamaterials*, vol. 5, pp. 178–205, 2011.

[60] G. V. Belokopytov, A. V. Zhuravlev, and Y. E. Terekhov, “Transmission of an electromagnetic wave through a bianisotropic metafilm”, *Phys. Wave Phenom.*, vol. 19, pp. 280–286, 2011.

[61] A. I. Dimitriadis, D. L. Sounas, N. V. Kantartzis, C. Caloz, and T. D. Tsiboukis, “Surface susceptibility bianisotropic matrix model for periodic metasurfaces of uniaxially mono-anisotropic scatterers under oblique TE-wave incidence”, *IEEE Trans. Antennas Propag.*, vol. 60, pp. 5753–5767, 2012.

[62] A. I. Dimitriadis, N. V. Kantartzis, and T. D. Tsiboukis, “Consistent modeling of periodic metasurfaces with bianisotropic scatterers for oblique TE-polarized plane wave excitation”, *IEEE Trans. Magn.*, vol. 49, pp. 1769–1772, 2013.

[63] A. I. Dimitriadis, N. V. Kantartzis, T. D. Tsiboukis, and C. Hafner, “Generalized non-local surface susceptibility model and Fresnel coefficients for the characterization of periodic metafilms with bianisotropic scatterers”, *Journal of Computational Physics*, vol. 281, pp. 251–268, 2015.

[64] A. N. Serdyukov, I. V. Semchenko, S. A. Tretyakov, and A. Sihvola, *Electromagnetics of bi-anisotropic materials: Theory and applications*, Amsterdam, The Netherlands: Gordon and Breach, 2001.

[65] Y. Ra'di, C. R. Simovski, and S. A. Tretyakov, "Thin perfect absorbers for electromagnetic waves: Theory, design, and realizations", *Phys. Rev. Applied*, vol. 3, no. 3, p. 037001, 2015.

[66] C. M. Watts, X. Liu, and W. J. Padilla, "Metamaterial electromagnetic wave absorbers", *Adv. Mater.*, vol. 24, no. 23, pp. OP98–OP120, 2012.

[67] W. Wan, Y. Chong, L. Ge, H. Noh, A. D. Stone, and H. Cao, "Time-reversed lasing and interferometric control of absorption", *Science*, vol. 331, no. 6019, pp. 889–892, 2011.

[68] V. Klimov, S. Sun, and G. -Y. Guo, "Coherent perfect nanoabsorbers based on negative refraction", *Opt. Expr.*, vol. 20, no. 12, pp. 13071–13081, 2012.

[69] S. Longhi, "Coherent perfect absorption in a homogeneously broadened two-level medium", *Phys. Rev. A*, vol. 83, no. 12, p. 055804, 2011.

[70] V. S. Asadchy, I. A. Faniayeu, Y. Ra'di, S. A. Khakhomov, I. V. Semchenko, and S. A. Tretyakov, "Broadband reflectionless metasheets: Frequency-selective transmission and perfect absorption", *Phys. Rev. X*, vol. 5, no. 3, p. 031005, 2015.

[71] W. T. Doyle, "Optical properties of a suspension of metal spheres", *Phys. Rev. B*, vol. 39, p. 9852, 1989.

[72] CST Studio Suite, 2013: http://www.cst.com.

[73] V. K. Varadan, V. V. Varadan, and A. Lakhtakia, "On the possibility of designing anti-reflection coatings using chiral composites," *J. Wave-Material Interaction,* vol. 2, no. 1 pp. 71–81, 1987.

[74] D. L. Jaggard, N. Engheta, and J. Liu, "Chiroshield: a Salisbury/Dallenbach shield alternative," *Elec. Lett.,* vol. 26, no. 17, pp. 1332–1334, 1990.

[75] B. Wang, T. Koschny, and C. M. Soukoulis, "Wide-angle and polarization-independent chiral metamaterial absorber," *Phys. Rev. B,* vol. 80, no. 3, p. 033108, 2009.

[76] C. F. Bohren, R. Luebbers, H. S. Langdon, and F. Hunsberger, "Microwave-absorbing chiral composites: Is chirality essential or accidental?," *Appl. Opt.,* vol. 31, no. 30, pp. 6403–6407, 1992.

[77] C. R. Brewitt-Taylor, "Modeling of helix-loaded chiral radar-absorbing layers," *PIER,* vol. 09, pp. 289–310, 1994.

[78] J. H. Cloete, M. Bingle, and D. B. Davidson, "The Role of chirality and resonance in synthetic microwave absorbers," *AEU-Int. J. Electron. Commun.,* vol. 55, no. 4, pp. 233–239, 2001.

[79] M. Yazdi, M. Albooyeh, R. Alaee, V. Asadchy, N. Komjani, C. Rockstuhl, C. Simovski, and S. Tretyakov, "A bianisotropic metasurface with resonant asymmetric absorption", *IEEE Trans. Antennas Propag.*, vol. 63, no. 7, pp. 3004–3015, 2015.

[80] D. Sievenpiper, L. Zhang, R. F. J. Broas, N. G. Alexópolous, and E. Yablonovitch, "High-impedance electromagnetic surfaces with a forbidden frequency band", *IEEE Trans. Microw. Theory Tech.*, vol. 47, no. 11, pp. 2059–2074, 1999.

[81] C. R. Simovski, M. Kondratiev, and S. He, "An explicit method for calculating the reflection from an anti-reflection structure involving array of C-shaped wire elements," *Journal of Electromagnetic Waves and Applications*, vol. 14, no. 10, pp. 1335–1352, 2000.

[82] F. Bilotti, A. Toscano, K. B. Alici, E. Ozbay, and L. Vegni, "Design of miniaturized narrowband absorbers based on resonant-magnetic inclusions," *IEEE Trans. Antennas Propag.*, vol. 53, no. 1, pp. 63–72, 2011.

[83] V. V. Yatsenko, S. I. Maslovski, S. A. Tretyakov, S. L. Prosvirnin, and S. Zouhdi, "Plane-wave reflection from double arrays of small magnetoelectric scatterers", *IEEE Trans. Microw. Theory Tech.*, vol. 51, no. 1, pp. 2–11, 2003.

[84] G. Kirchhoff, "Zur Theorie der Lichtstrahlen", *Annal. Phys.*, vol. 254, no. 4, pp. 663–695, 1883.

[85] A. Alù and N. Engheta, "Pairing an epsilon-negative slab with a mu-negative slab: Resonance, tunneling and transparency," *IEEE Trans. Antennas Propag.,* vol. 51, no. 10, pp. 2558–2571, 2003.

[86] D. L. Gao, L. Gao, and C. W. Qiu, "Birefringence-induced polarization-independent and nearly all-angle transparency through a metallic film," *EPL,* vol. 95, no. 3, p. 34004, 2011.

[87] F. Monticone, C. Valagiannopoulos, and A. Alù, "Aberration-free planar focusing based on parity-time symmetric nonlocal metamaterials," in *IEEE International Symposium on Antennas and Propagation and North American Radio Science Meeting,* Vancouver, Canada, 2015, pp. 252–253.

[88] S. A. Tretyakov, "Uniaxial omega medium as a physically realizable alternative for the perfectly matched layer (PML)", *Journal of Electromagnetic Waves and Applications*, vol. 12, pp. 821–837, 1998.

[89] S. D. Gedney, "An anisotropic perfectly matched layer – absorbing medium for the truncation of FDTD lattices," *IEEE Trans. Antennas Propag.*, vol. 44, no. 12, pp. 1630–1639, 1996.

[90] L. Zhou, W. Wen, C. T. Chan, and P. Sheng, "Electromagnetic-wave tunneling through negative-permittivity media with high magnetic fields," *Phys. Rev. Lett.,* vol. 94, no. 24, p. 243905, 2005.

[91] G. Castaldi, V. Galdi, A. Alù, and N. Engheta, "Electromagnetic tunneling of obliquely incident waves through a single-negative slab paired with a double-positive uniaxial slab," *J. Opt. Soc. Am. B,* vol. 28, no. 10, pp. 2362–2368, 2011.

[92] T. Feng, Y. Li, H. Jiang, Y. Sun, L. He, H. Li, Y. Zhang, Y. Shi, and H. Chen, "Electromagnetic tunneling in a sandwich structure containing single negative media," *Phys. Rev. E,* vol. 79, no. 2, p. 026601, 2009.

[93] Z. Lin, H. Ramezani, T. Eichelkraut, T. Kottos, H. Cao, and D. N. Christodoulides, "Unidirectional invisibility induced by $\mathcal{PT}$-symmetric periodic structures", *Phys. Rev. Lett.*, vol. 106, p. 213901, 2011.

[94] R. Fleury, D. L. Sounas, and A. Alù, "Negative refraction and planar focusing based on parity-time symmetric metasurfaces", *Phys. Rev. Lett.*, vol. 113, p. 023903, 2014.

[95] A. Regensburger, C. Bersch, M. -A. Miri, G. Onishchukov, D. N. Christodoulides, and U. Peschel, "Parity-time synthetic photonic lattices", *Nature*, vol. 488, pp. 167–171, 2012.

[96] D. L. Sounas, R. Fleury, and A. Alù, “Unidirectional cloaking based on metasurfaces with balanced loss and gain,” *Phys. Rev. Appl.,* vol. 4, no. 1, p. 014005, 2015.

[97] W. W. Salisbury, “Absorbent body of electromagnetic waves”, U.S. Patent 2 599 944 (10 June 1952).

[98] W. Dallenbach and W. Kleinsteuber, “Reflection and absorption of decimeter-waves by plane dielectric layers”, *Hochfreq. u Elektroak*, vol. 51, pp. 152-156, 1938.

Errata

Publication II

There are misprints in equations (1) and (2). The correct form of these equations read as follows:

$$E_{\text{forward}} = \frac{-j\omega}{2S}\left(\eta_0 p + m\right), \quad E_{\text{back}} = \frac{-j\omega}{2S}\left(\eta_0 p - m\right)$$

The rest of the discussions and results in the paper remain unaffected.

Publication VI

In addition to the teleportation phenomenon which happens at the resonance frequency of the presented structures, a huge amplification may happen in transmission which is of tunneling nature. Depending on the reactance of the inductive layers, this high-amplitude tunneling phenomenon can occur at frequencies close or far from the teleportation frequency. Similar phenomenon happens when we deviate the angle of incidence from the designed value. A detailed investigation will be subject of another study.

The thesis is devoted to metasurfaces, which are composite layers designed to manipulate electromagnetic waves. The appeal of these functional metasurfaces lies in their ability to control the flow of electromagnetic waves in electrically thin planar structures. This thesis studies different functional metasurfaces such as off-band-transparent absorbing metasurfaces, off-band-transparent reflecting metasurfaces, Huygens' metasurfaces, and parity-time-symmetric teleportation devices. It also indicates likely research avenues for the future.

Aalto-DD 211/2015

ISBN 978-952-60-6566-3 (printed)
ISBN 978-952-60-6567-0 (pdf)
ISSN-L 1799-4934
ISSN 1799-4934 (printed)
ISSN 1799-4942 (pdf)

Aalto University
School of Electrical Engineering
Department of Radio Science and Engineering
www.aalto.fi

BUSINESS + ECONOMY

ART + DESIGN + ARCHITECTURE

SCIENCE + TECHNOLOGY

CROSSOVER

DOCTORAL DISSERTATIONS